Received: 25 May 2024 | Accepted: 16 December 2024

DOI: 10.1111/1365-2435.14751

Functional Ecology

RESEARCH ARTICLE

Divergence of vessel diameter explains interspecific variation in hydraulic safety to salinity in the Sundarbans mangrove ecosystem

Md. Qumruzzaman Chowdhury[1] | Swapan Kumar Sarker[1] | Md. Imam Hossain Imran[1] | Anup Datta[1] | Syeda Kaifee Akhter[1] | Zubayer Ahmed[1] | Hans Beeckman[2]

[1]Department of Forestry and Environmental Science, Shahjalal University of Science and Technology, Sylhet, Bangladesh

[2]Service of Wood Biology, Royal Museum for Central Africa (RMCA), Tervuren, Belgium

Correspondence
Md. Qumruzzaman Chowdhury
Email: qumrul-for@sust.edu

Funding information
SUST Research Center, Grant/Award Number: FES/2021/2/03 and FES/2020/1/05

Handling Editor: Antonella Gori

Abstract

1. Despite their crucial role in providing ecosystem services and livelihood support in 124 countries, mangroves are facing challenges from warming, altered seasonal precipitation and sea level rise (SLR) in the face of climate change. Variation in intra- and interspecific hydraulic traits and related xylem anatomy may allow trees to adapt to changing environmental conditions, yet little is known about adaptive plasticity in mangroves.
2. We examined (i) xylem and hydraulic trait variation across three (low, medium and high) salinity zones in three widespread mangrove species (*Exocecaria agallocha*, *Xylocarpus moluccensis* and *Heritiera fomes*) with distinct shade tolerance characteristics in the Bangladesh Sundarbans, (ii) associations of xylem and hydraulic traits, and (iii) habitat (regulator, resource and forest structure) effects on vessel diameter due to its strong influence on hydraulic conductivity variation.
3. Although potential conductivity (K_P) and leaf-specific conductivity (K_L) showed species-specific variation, a notably greater conductivity was found in the low-salinity zone (LSZ), which had lower vessel wall reinforcement $(t/b)^2$. Xylem and hydraulic traits exhibited mostly strong phylogenetic signals, whereas pairwise relationships between traits were phylogenetically independent. The study species had distinct hydraulic characteristics, where vessel diameter (*D*) was strongly related to the variation in K_P and K_L. Furthermore, the study species exhibited a weak trade-off between hydraulic efficiency and safety.
4. A greater percentage of smaller vessel diameters in light-demanding *E. agallocha* indicates greater hydraulic safety against cavitation under stressful conditions than in shade-tolerant *H. fomes*, followed by *X. moluccensis*. Although species characteristics place broad bounds on xylem traits, the combined effects of salinity, nutrient availability and tree size modulate vessel diameter, which leads to hydraulic conductivity variation.

This is an open access article under the terms of the Creative Commons Attribution License, which permits use, distribution and reproduction in any medium, provided the original work is properly cited.
© 2025 The Author(s). *Functional Ecology* published by John Wiley & Sons Ltd on behalf of British Ecological Society.

5. The contrasting safety in terms of vessel diameter in mangroves suggests an important role in adaptation to salinity and species distribution. The results also provide insight into salinity-induced growth reduction and mortality in mangroves.

KEYWORDS
hydraulic conductivity, mangrove, safety–efficiency trade-off, salinity, shade tolerance, the Sundarbans, xylem anatomy

1 | INTRODUCTION

Along with livelihood support to millions of coastal people living in 124 (sub)tropical countries, mangroves are carbon-rich intertidal ecosystems provide valuable cultural, provisioning, regulating and supporting services (Krauss & Osland, 2020; Song et al., 2023; Spalding & Leal, 2021). By maintaining extremely low xylem water potentials and reducing water loss, mangrove tree species extract water through various xylem structural and physiological adaptations to survive in saline environment (Gauthey et al., 2022; Krauss et al., 2008; Nguyen et al., 2017; Reef & Lovelock, 2015; Schmitz, Egerton, et al., 2012a; Schmitz, Koch, et al., 2012b). Hydraulic conduction is challenging in mangroves because salinity causes less capillary water transport, which eventually leads to salinity-induced drought stress (Raza et al., 2023). Climate change consequences, such as sea level rise (SLR), rising temperature and atmospheric vapour pressure deficit (VPD), create additional stress on mangrove tree hydraulic systems (Friess et al., 2022; Reef & Lovelock, 2015). As physiological drought intensifies, tension in the xylem increases, thus increasing the probability of cavitation in conductive cells, such as embolism formation in vessels (Cochard et al., 2013; Jiang et al., 2021; Lens et al., 2022; Tyree & Sperry, 1989). This phenomenon can eventually lead to systemic failure of water transport systems and, as a result, tree die-offs (Brodribb & Cochard, 2009; Gauthey et al., 2022; McDowell et al., 2008). Therefore, a clear understanding of how hydraulic functioning changes in mangrove tree species under salinity stress is essential for better management and conservation of threatened mangrove ecosystems.

Hydraulic traits (e.g. hydraulic conductivity and vessel wall reinforcement) play a critical role in shaping species distributions and functions in a wide range of ecosystems, including mangroves (Blackman & Brodribb, 2011; Cosme et al., 2017; Jiang et al., 2017; Jiang et al., 2021; Laughlin et al., 2020; Madrid et al., 2014; Oliveira et al., 2019; Robert et al., 2009; Schmitz et al., 2006). Trees require a certain level of water transport for photosynthesis and transpiration, as well as adequate mechanical support, to withstand physical damage (Lachenbruch & McCulloh, 2014; Onoda et al., 2010; Wagner et al., 1998). However, mangrove species are likely to have conservative resource acquisition strategies and are unlikely to require a high degree of hydraulic efficiency to sustain photosynthesis (Ball, 1996; Jiang et al., 2021; Oliveira et al., 2021; Sobrado, 2001). Therefore, studies focusing on a diverse range of species across salinity gradients can aid in understanding the tree hydraulic mechanisms in stressful mangrove environments.

Potential hydraulic conductivity (K_P) can quantify the water transport ability in the xylem, whereas leaf-specific hydraulic conductivity (K_L) indicates the hydraulic efficiency of xylem to supply water per unit of transpiration area (Bittencourt et al., 2016; Sperry & Tyree, 1988). Among the xylem traits, vessels conduct water where fibres support mechanical strength, and a trade-off between hydraulic efficiency (more conductive area) and mechanical safety (dense wood) has been suggested (Pratt & Jacobsen, 2017). Such a trade-off, however, might be regulated by altered vessel area in sapwood (the proportion of water-conducting vessel area, *F*), vessel composition (*S*, an index of narrow to wide vessel lumens) and the ratio of sapwood area to leaf area. In addition to pit membrane characteristics, vessel lumen diameter (henceforth vessel diameter, *D*) is a strong determinant of hydraulic efficiency (Jacobsen & Pratt, 2023). Both *D* and hydraulic conductivity tend to decrease with increasing environmental stress, such as salinity in mangroves (Madrid et al., 2014; Robert et al., 2009; Schmitz et al., 2007; Sobrado, 2007; Verheyden et al., 2004). In contrast, smaller vessels lead to greater hydraulic safety because of the lower risk of cavitation, as small vessels have a lower risk of air-seeding due to a smaller pit membrane area (Hacke et al., 2006; Schmitz et al., 2012b). In addition, higher vessel grouping may have functional advantages in hydraulic conduction. For example, group vessels facilitate hydraulic transport, bypassing embolized vessels through the intervessel pits of close neighbouring vessels (Baas et al., 1983; López-Portillo et al., 2005; Robert et al., 2009; Yáñez-Espinosa et al., 2001). Furthermore, vessels require greater structural reinforcement in vessel walls $(t/b)^2$ to avoid hydraulic stress (vessel cavitation) at low water potentials (high tension), especially under stressful environmental (saline) conditions (Hacke, 2015; Janssen et al., 2020; Jiang et al., 2022). Therefore, the ability of different tree species to adapt to diverse stress conditions, for example salinity depends on plasticity of the hydraulic-related xylem traits.

Xylem traits are heritable and sensitive to evolutionary modifications (Carlquist, 2012). Compared with distantly related species, family-level phylogenetic studies suggest that more closely related species under specific environmental conditions have more similar xylem traits (Carvalho et al., 2023; Chave et al., 2006; Zanne et al., 2018). Instead, the lack of phylogenetic signals could imply evolutionary lability (Arenas-Navarro et al., 2021). Differences in xylem and hydraulic traits along environmental gradients can influence

tree function, leading to interspecific variation (Li et al., 2023; Rosas et al., 2019; Savva et al., 2010). Phylogenetic signals for hydraulic traits are much weaker than those for xylem traits (Hietz et al., 2017). This means that evolution is likely to have less of an effect on them than on vessel size and number.

Nonetheless, xylem traits have established conceptual frameworks to address ecological questions (Beeckman, 2016), and we still lack a general understanding of how xylem hydraulic trait variation is linked to the environmental stresses that underlie species survival, growth and distribution, particularly in mangroves. In mangroves, tree growth and distribution are influenced by the interaction of different habitat variables, such as regulators (e.g. soil salinity and siltation), resources (e.g. nutrients) and forest structure (e.g. DBH, height and tree density; Chowdhury, Sarker, Sultana, et al., 2023; Sarker et al., 2021; Twilley & Rivera-Monroy, 2005). These variables may put selective pressure on the trade-offs or associations among xylem traits to shape hydraulic functions in trees. For example, tree species from stressful salinity areas tend to have narrower vessels and thus greater resistance to cavitation but lower hydraulic conductivity than those from low-salinity areas (Pockman & Sperry, 2000; Robert et al., 2009; Schmitz et al., 2006). Furthermore, light-demanding species may have different hydraulic strategies than shade-tolerant species to regulate hydraulic flows for survival, growth and distribution. Although mangrove hydraulic studies have focused mainly on understanding the effects of soil salinity, siltation and nutrients on a few mangrove species, such as *Avicennia* sp., *Ceriops* sp., *Laguncularia* sp. and *Rhizophora* sp. (De Deurwaerder et al., 2016; Lovelock et al., 2006; Madrid et al., 2014; Okello et al., 2017; Robert et al., 2009; Schmitz et al., 2007; Sobrado, 2006), little is known about how hydraulic properties are related to the shade tolerance of species. All hydraulic traits are likely to be strongly affected by the interactive effects of habitat variables, as described for growth and morphological trait variation in mangrove species (Chowdhury, Sarker, Sultana, et al., 2023; Sarker et al., 2021). However, tree responses to multiple interactive stresses cannot be inferred from a single stress (Li et al., 2023; Suzuki et al., 2014). Therefore, quantifying the interactive effects of these factors is crucial for predicting mangrove species responses to future environmental changes.

Sundarbans, the largest single block of mangroves (~10,000 km^2) on Earth, safeguards the coasts and lives and sustain livelihoods in two neighbouring South Asian countries, Bangladesh and India (Ahmed, Sarker, Friess, et al., 2023; Gopal & Chauhan, 2018). Although this Ramsar and UNESCO World Heritage Site harbours relatively high floral diversity, including the IUCN listed globally endangered species, for example *Heritiera fomes* Buch.—Ham., the ecosystem is largely threatened by anthropogenic disturbances and environmental changes in the face of climate change (Dasgupta et al., 2017; Sarker et al., 2019; Ward et al., 2016). Furthermore, higher rates of SLR and sedimentation limit tree growth and change species distributions in the Sundarbans (Ahmed, Sarker, Friess, et al., 2023; Sarker et al., 2016), which can affect hydraulic functioning in trees (e.g. Okello et al., 2017). However, a basic understanding of the hydraulic architecture of surviving mangrove tree species in the Sundarbans is scarce.

In this study, we investigated the xylem and hydraulic traits of three widely distributed tree species in the Bangladesh Sundarbans. Among them, *Excoecaria agallocha* L. (Euphorbiaceae) is a light-demanding species that grows on the coasts of the Indo-West Pacific (IWP) (Reef & Lovelock, 2015). The shade-bearing *Xylocarpus moluccensis* Pierre (Meliaceae) grows in the West Pacific (WP) and *H. fomes* (Sterculiaceae) is distributed in the Indo-Malaysian (IM) mangroves. An earlier study (Sarker et al., 2019) revealed a declining population growth of these species (especially in higher salinity areas) in the Sundarbans, similar to global trends (Polidoro et al., 2010). This study aimed to (i) identify the species-specific variation in xylem and hydraulic traits across salinity gradients, (ii) determine the associations between xylem and hydraulic traits, and (iii) understand the effects of habitat conditions (regulators, resources and forest structure) on one of the most important xylem traits, the vessel diameter (Jacobsen & Pratt, 2023) that regulates hydraulic conductivity variation.

2 | MATERIALS AND METHODS

2.1 | Study site

The study was conducted at the Bangladesh Sundarbans (21°30′–22°30′ N, 89°00′–89°55′ E; Figure 1a), which is located in the estuary of the Ganges-Brahmaputra River system. It covers 6017 km^2 area, 31% of which is composed of water bodies, such as rivers, canals and small streams (Sarker et al., 2016; Siddique et al., 2021). The forest is inundated twice a day with 3–4 m high tides (Islam & Gnauck, 2011), and the sedimentation rate is high (~2.4 billion tons of sediments $year^{-1}$; Mitra & Zaman, 2016).

Salinity is an important regulatory factor in this ecosystem that varies both spatially and seasonally (Ahmed, Sarker, Friess, et al., 2023; Chowdhury, Sarker, Hossain, et al., 2024; Sarker et al., 2021). Based on spatial salinity variation, this ecosystem is divided into three contrasting salinity zones: low-salinity zone (LSZ, eastern and north-eastern part), medium salinity zone (MSZ, central and southern part) and high salinity zone (HSZ, western and south-western part) (Sarker et al., 2016). In addition to tides from the Bay of Bengal, precipitation and freshwater discharge from the upstream river (the Ganges) regulate the spatial and seasonal variation in salinity (Chowdhury, Sarker, Gupta, & Datta, 2023). During the monsoon (June–September), salinity decreases due to increased precipitation and increased freshwater flow from the Ganges, and salinity increases steadily after freshwater flows are reduced during the post-monsoon (October–November), followed by winter (December–February) and pre-monsoon (March–May) (Chowdhury, Sarker, Gupta, & Datta, 2023; Figure 1b). Furthermore, after commissioning the Farakka barrage in India in 1975, the salinity increased by 60% because of a decrease in fresh water discharge from the Ganges (Aziz & Paul, 2015). The region is characterized by a monsoonal

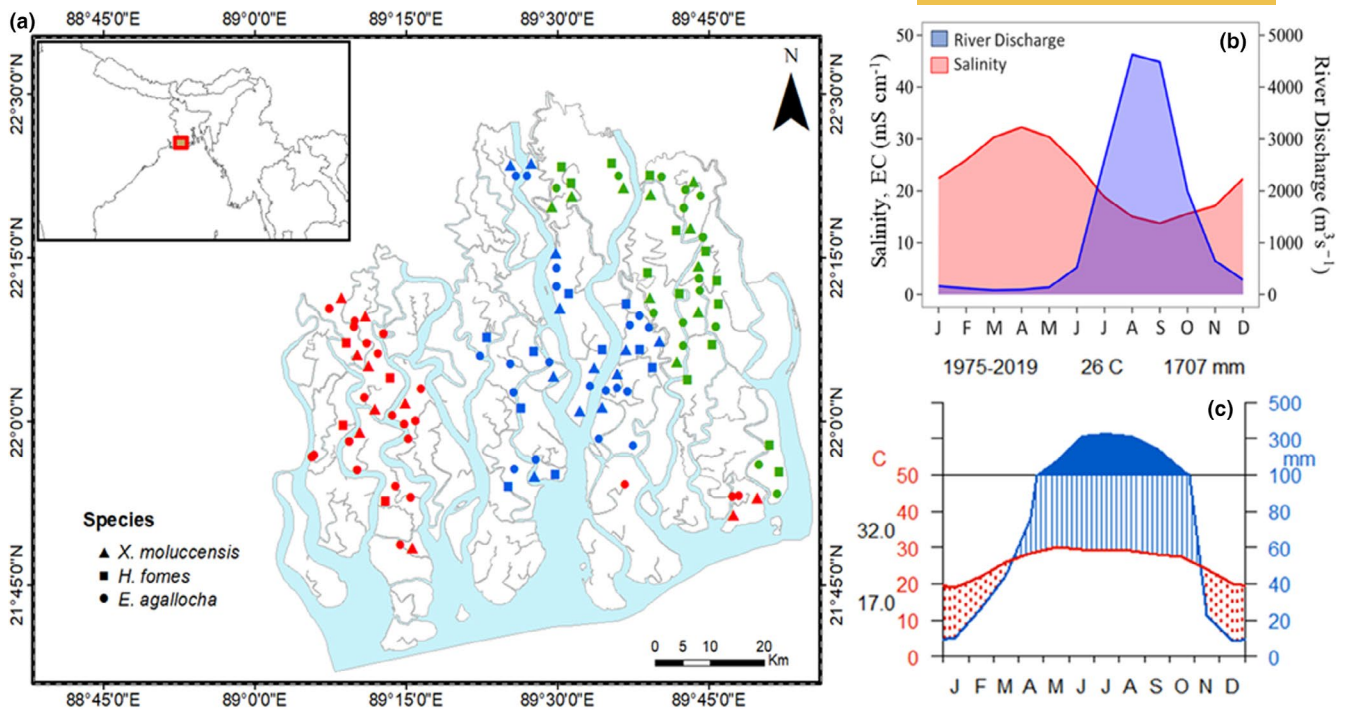


FIGURE 1 Sampling locations in three salinity zones in the Bangladesh Sundarbans (a). The green colour, the low (LSZ); the blue colour, the medium (MSZ); the red colour, the high salinity zone (HSZ). Intra-annual mean salinity (EC, electrical conductivity, mS cm^{-1}) and mean river discharge ($m^3 s^{-1}$) variation (b). Intra-annual mean precipitation, mm and mean temperature, °C variation (c). Dry winter (December–February), pre-monsoon (March–May), monsoon (June–September) and post-monsoon (October–November).

climate (Figure 1c), where the mean annual rainfall is 1700 mm (ranging from 1474 to 2265 mm) and the mean temperature ranges from 20 to 30°C (Chowdhury, Sarker, Sultana, et al., 2023).

The Bangladesh Sundarbans is a *H. fomes* dominated uneven-aged mangrove ecosystem (Sarker et al., 2016). It comprises different size classes of *E. agallocha*, *X. moluccensis*, *Bruguiera gymnorrhiza* (L.) Lam., *Ceriops decandra* (Griff.) Ding Hou, *Cynometra ramiflora* L. in association with *H. fomes* (Hossain, 2015). Such species compositions vary spatially across salinity gradients, particularly in high salinity areas, where most of the species have disappeared. For example, *H. fomes* prefers freshwater dominated habitats and has a negative response to increased soil salinity (Chowdhury, De Ridder, et al., 2016; Sarker et al., 2016). The *H. fomes* population is estimated to have declined by 76% since 1959, mainly due to excessive harvesting and top-dying disease (Iftekhar & Saenger, 2008; Sarker et al., 2019). Although the distribution of *X. moluccensis* is decreasing because of overharvesting (Sarker et al., 2016), *E. agallocha* is still widely distributed across the Sundarbans due to its salt tolerance and regeneration characteristics, with a greater ability to colonize open and degraded habitats (Harun-or-Rashid et al., 2009; Sarker et al., 2016).

2.2 | Tree selection, measurements and sample collection

Compared with other tree species in the Sundarbans (Sarker et al., 2021), the most dominant *H. fomes*, the second most dominant *E. agallocha* and dominant *X. moluccensis* were selected for sampling. Since 1986, the Bangladesh Forest Department (BFD) has established a total of 120 permanent sample plots (PSPs; size, 0.2 ha with dimensions of 100 × 20 m) in the Sundarbans for biodiversity and forest stock monitoring (Chowdhury, Kitin, et al., 2016; Sarker et al., 2016, 2019). In this study, a total of 60 PSPs were selected for sampling in three contrasting salinity zones (i.e. the LSZ, MSZ and HSZ; Figure 1a). To avoid seasonal harsh weather conditions, such as heavy monsoonal precipitation, storms and excessive tidal surges, we performed field measurements and sampling from December to April (2020–2021) under the permission of the BFD (permit no.: BFD-22.01.0000.004.04.21.1.20.588, dated 13 December 2020). All trees with DBH ≥4.5 cm (at a height of 1.3 m from the ground) were measured to calculate stand characteristics, such as tree density (stem ha^{-1}). The DBH (cm) and tree height (m), were measured using a diameter tape and a Suunto clinometer (Suunto, Vantaa, Finland), respectively. We also quantified the coefficient of variation of DBH (CoV DBH) and tree height (CoV H), which indicates tree size inequality in the PSPs (Chen et al., 2023).

Based on the availability of the study tree species, one to three trees were purposively selected from each PSP for wood core and leaf collection. Wood cores were collected at a height of 1.3 m above the ground with an increment borer (diameter, 4.3 mm; Haglöf, Sweden). The third order fully expanded leaf pair from the apex of the plagiotropic (lateral) branches was selected for sampling. We avoided leaves with obvious symptoms of pathogen or herbivore attack or with a substantial cover of epiphylls. In that case, we

measured the fourth order leaves of the branches. Afterwards, the wood cores and leaves were placed in polythene bags separately for laboratory analyses. We measured the fresh area of the leaves using images (captured by a digital camera, Nikon D5500; Nikon, Tokyo, Japan) in Adobe Photoshop CS (Adobe, San Jose, California, USA) following Sarker et al. (2021). The soil samples from each PSP were collected at a depth of 15 cm using a 5 cm diameter cylindrical soil core sampler for laboratory analysis (Sarker et al., 2016). A total of nine soil samples were collected (1 from each corner, 1 from the middle of each side and 1 from the centre of the rectangular PSP), and subsequently, all the samples were mixed together to make one composite soil sample for the PSP. The soil samples were stored in polythene bags for laboratory analyses.

2.3 | Site variable analysis

We selected regulatory variables, such as soil salinity, silt percentage, pH and elevation because of their critical roles in tree growth and distribution in the Sundarbans (Chowdhury, Sarker, Sultana, et al., 2023; Sarker et al., 2016). The collected composite soil samples were used for these analyses. The soil salinity (EC, $mS\,cm^{-1}$) was measured using a digital conductivity meter (Extech 341350A-P Oyster) at a 1:5 ratio in a suspension of soil in water (Hardie & Doyle, 2012). A digital pH meter (Extech RE300 ExStik) was used to measure the soil pH. The soil texture (silt percentage) was analysed using the hydrometer method (Gee & Bauder, 1986). Highly dynamic regional hydrology influences sediment deposition in the Sundarbans and, consequently, at variable elevations, even within a small distance (<1 km; Sarker et al., 2016). Five elevation readings were randomly extracted from each PSP from the digital elevation model (DEM), and these readings were averaged for each PSP to reduce the errors associated with the DEMs (Sarker et al., 2021).

We selected resource variables, such as soil NH_4, P and K because of their important influences on mangrove tree growth and development (Reef et al., 2010). Soil NH_4 was measured following the Kjeldahl method (Bremner & Breitenbeck, 1983). We followed the molybdovanadate method to measure the soil P concentration (Ueda & Wada, 1970). The total soil K was determined using an atomic absorption spectrophotometer (AA-7000).

2.4 | Wood anatomical analysis

2.4.1 | Microtomy and microscopy

Owing to the age trend in vessel characteristics in mangrove tree species (Chowdhury et al., 2008; Schmitz et al., 2006; Siddique et al., 2021), we used the outer part of the wood core (near bark) from each tree for microtomy. Wood sections of 15 μm in thickness were cut using a microtome (HistoCore AUTOCUT, Leica, Germany). Afterwards, the sections were stained in a solution of 0.1% safranin (Merck KGaA, Darmstadt, Germany) and 50% ethanol. The sections were subsequently washed for 5 min in 50%, 75%, 96% and 100% ethanol series and subsequently mounted on microscopic slides (Chowdhury, Kitin, et al., 2016). Observations were performed under a light microscope, and images were captured using a camera system connected to the microscope.

2.4.2 | Xylem trait measurements

The microscopic images were analysed using Fiji ImageJ software (Schindelin et al., 2012). We used five 500 μm resolution images for vessel density (VD) measurements for each tree using the following equation:

$$\mathrm{VD} = \text{number of vessels} / \text{area}\ \left(\mathrm{mm}^2\right)$$

The vessel diameter, D (both tangential and radial, μm), was measured on the images. We randomly measured the diameters of 100 vessels for each tree. We also used the images to calculate the vessel grouping index (GI) and then averaged the values in each case. The GI is a measure of vessel aggregation in cross sections (Lens et al., 2011), which improves resilience to embolism through the redundancy of hydraulic pathways (von Arx et al., 2013). The GI was calculated as the ratio of the total number of vessels to the total number of vessel groupings in each image (Scholz et al., 2013).

The proportion of water-conducting vessel area (F) and vessel composition index (S, mm^4) for each tree were also calculated following the following equations (Hacke et al., 2001; Zanne et al., 2010):

$$\mathrm{F} = \mathrm{VA} \times \mathrm{VD}$$

$$\mathrm{S} = \mathrm{VA} / \mathrm{VD}$$

where VA indicates the mean vessel area, and VD indicates the mean vessel density.

2.4.3 | Hydraulic trait calculations

Based on the Hagen–Poiseuille law, the hydraulically weighted diameter (D_H, μm) was calculated using a statistic that weights the vessel lumen size (Sperry et al., 1994).

$$D_H = \Sigma D^5 / \Sigma D^4.$$

Hagen–Poiseuille's law was also used to determine potential conductivity (K_p, $kg\,m^{-1}\,MPa^{-1}\,s^{-1}$) based on hydraulic diameter (D_H) and VD.

$$\mathrm{K_p} = \left(\frac{\pi\rho}{128\eta}\right) * D_H^4 * VD$$

where η is the viscosity index of water (1.002×10^{-9} MPa s at 20°C); ρ is the density of water at 20°C (998.21 $kg\,m^{-3}$); D is the vessel diameter (μm).

Leaf-specific conductivity (K_L, kg m^{-1} MPa^{-1} s^{-1}) was calculated as the ratio of potential conductivity (K_p) to leaf area (LA) (Tyree & Zimmermann, 2002).

The double wall thickness (μm) was measured for 50 pairs of interconnected vessels on each tree to determine the mean thickness. The vessel wall reinforcement $(t/b)^2$ indicates the capacity of vessels to resist water pressure deficit and was calculated as the ratio of the paired vessel wall thickness (t) and the diameter of the vessel closest to the hydraulic mean diameter (b) following Hacke et al. (2001) and Pittermann et al. (2006).

2.5 | Statistical analysis

The Shapiro–Wilk normality test was performed to check the normality of the data. In the case of normality, the xylem and hydraulic trait variations among the salinity zones (LSZ, MSZ and HSZ) and among the species were analysed using one-way analysis of variance (ANOVA) followed by a post hoc (Tukey) test; otherwise, a nonparametric (Kruskal–Wallis) test followed by a post hoc (Dunn's) test was used. In the absence of normality, log-transformed data were used for other analyses. We performed principal component analysis (PCA) to test the associations among the studied hydraulic and xylem traits. The factor analysis of mixed data (FAMD) method was used to perform PCA using the 'FactoMineR' package (Lê et al., 2008). All the analyses were performed in the R platform (R Core Team, 2023).

To assess the presence of phylogenetic signals in xylem and hydraulic traits, we calculated Blomberg's *K*-values using the 'phylosig' function from the 'phytools' package in R (Revell, 2012). Blomberg's *K*-value is a statistic that compares the observed trait variance across a phylogenetic tree to the variance expected under a Brownian motion model of trait evolution (Blomberg et al., 2003). A *K*-value >1 indicates that closely related species are more similar in their traits than expected under Brownian motion. This suggests a greater phylogenetic effect on the trait distribution. Conversely, a *K*-value <1 suggests a weaker phylogenetic signal, indicating that closely related species are less similar in their traits than expected and implying a weaker phylogenetic effect (Blomberg et al., 2003). Phylogenetic trees of the species were constructed on the basis of available phylogenetic information, ensuring congruence with the species included in our study. A phylogenetic signal was considered significant if the *p*-value from the randomization test was <0.05.

We calculated pairwise correlations using phylogenetically independent contrasts (PICs; Felsenstein, 1985) to investigate the phylogenetic effects in the dataset. We constructed a phylogenetic tree using the 'pbtree' function from the 'ape' package to ensure that it was rooted and fully dichotomous using the 'multi2di' function in R (R Core Team, 2023). We then used the 'pic' function from the 'picante' package to calculate the PICs for each variable. We subsequently computed pairwise Pearson correlation coefficients on the resulting PICs, and the significant correlations were identified by applying a threshold (e.g. $p < 0.05$).

We used generalized additive models (GAMs) to understand the combined effects of regulators, such as salinity, pH, silt %, elevation, resources (e.g. N, P and K) and forest structure (e.g. height, DBH, CoV height, CoV DBH and tree density) on vessel diameter in the studied species (Wood & Augustin, 2002). To evaluate the influence of each explanatory variable, the cubic spline 'cr' was used to delineate the predictor–response relationships. A nonparametric smoothing function was used with an effective degree of freedom using the 'mgcv' package version 1.8–41 (Wood, 2017) in R, version 4.3.1 (R Core Team, 2023).

With all possible combinations of variables, we fitted all possible candidate GAMs, and the models were ranked by the Akaike information criterion (AICc) using the 'dredge' function in the 'MuMIn' package version 1.47.5 in R (Bartoń, 2023; Burnham & Anderson, 2002). The ΔAICc represents the difference between the AICc value of the best model and the AICc values of the other models. We used a 'ΔAICc ≤2' criterion as a selection metric for the confidence set of the models. The relative contribution of each variable in the best-fitting model was evaluated by computing the AICcw values and the difference in total deviance explained between the entire model and the model with variables. Subsequently, AICc-weighted model averaging was applied to the parameter estimates of the selected models to mitigate model selection uncertainty and potential biases. To identify the key variables, we used the 'importance' function of the 'MuMIn' package by determining the strength of the covariates and ranking them based on their relative importance (RI). The RI values range from 0 to 1, where 0 indicates that the target covariate is excluded from all competing models, and 1 indicates inclusion in all competing models. We measured the goodness-of-fit of the models using the coefficient of determination (R^2) statistic between the observed and estimated values.

3 | RESULTS

3.1 | Hydraulic and xylem trait variation among the salinity zones

We compared the variation in hydraulic and xylem traits of the studied species among the salinity zones (Figure 2; Table 1). The soil salinity variation among three zones (the LSZ, 4.67 ± 2.25 mS cm^{-1}; the MSZ, 7.50 ± 2.50 mS cm^{-1} and the HSZ, 11.75 ± 1.86 mS cm^{-1}) was significant ($p < 0.05$). Although the mean potential conductivity (K_p) and leaf-specific conductivity (K_L) decreased from the LSZ to the HSZ, a significantly lower K_p was found in the HSZ in *E. agallocha* and *H. fomes* (Figure 2). Similarly, a significantly lower K_L was found in the HSZ only for *H. fomes*. Conversely, a significantly lower vessel wall reinforcement $(t/b)^2$ value was found in the LSZ (Figure 2).

Xylem traits related to hydraulic conductivity also varied among the salinity zones (Table 1). However, the xylem traits did not exhibit the same patterns of variation. For example, VD significantly differed among the salinity zones in the study species, except for *E. agallocha*, and the lowest value was in the LSZ in each

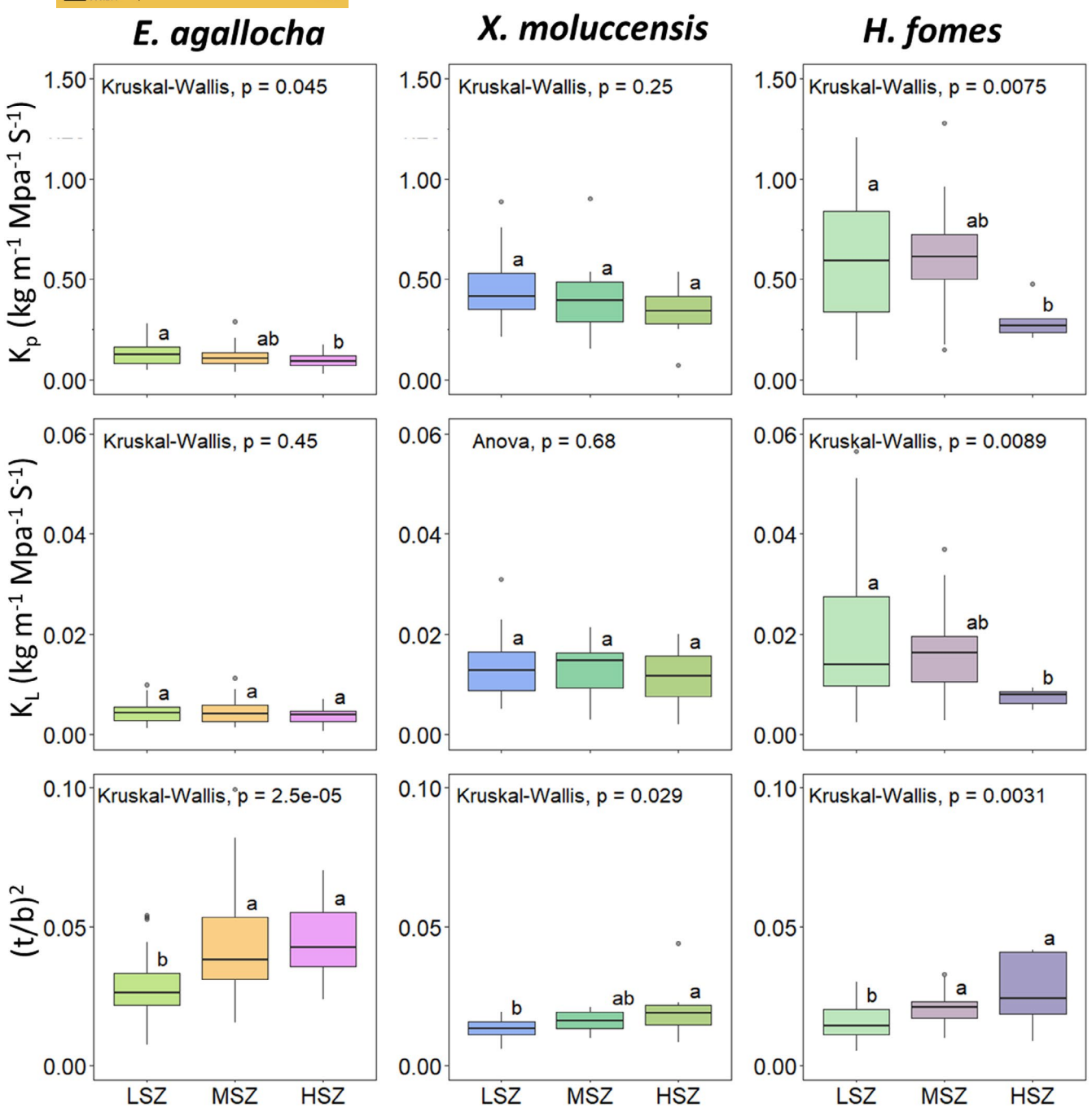


FIGURE 2 Hydraulic traits variation across the salinity gradients, that is the low (LSZ), the medium (MSZ) and the high salinity zone (HSZ) the Bangladesh Sundarbans. K_P, Potential conductivity; K_L, Leaf-specific conductivity; $(t/b)^2$, vessel wall reinforcement. Different letters denote statistically significant variation at $p < 0.05$ and same letter is not significant ($p < 0.05$).

case. In contrast, vessel diameter (*D*) and hydraulically weighted vessel diameter (D_H) were significantly lower in the HSZ than in the LSZ for each species (Table 1). The vessel composition index (*S*) indicates a greater contribution of wide vessels to water conduction in a given area (Zanne et al., 2010). A significantly greater *S* was found in the LSZ than in the HSZ in the study species, except for *X. moluccensis*. On the contrary, the proportion of water-conducting vessel area (*F*) was similar across the salinity gradients in each case. The vessel GI significantly varied among the salinity zones only in *H. fomes* (Table 1).

A comparison of species (the data were averaged for each species regardless of salinity zone) revealed that *E. agallocha* had significantly lower K_P and K_L values, whereas *H. fomes* had higher values (Figure 3A,B). On the contrary, a significantly higher $(t/b)^2$ was detected in *E. agallocha* than in *X. moluccensis* and *H. fomes* (Figure 3C).

TABLE 1 Tree characteristics and xylem traits variations among the salinity zones (i.e. the low-salinity zone, LSZ; the medium salinity zone, MSZ; the high salinity zone, HSZ) in the Sundarbans.

Species		Variables	LSZ (mean ± SD)	MSZ (mean ± SD)	HSZ (mean ± SD)
E. agallocha	Tree characteristics	Sample trees (N)	32	40	34
		Diameter at breast height, DBH (cm)	13.56 ± 3.06^{a}	13.64 ± 3.09^{a}	12.52 ± 3.75^{a}
		Tree height (m)	7.03 ± 1.87^{a}	6.69 ± 2.38^{a}	5.19 ± 1.56^{b}
		Leaf area, LA (cm^2)	29.88 ± 7.62^{a}	27.7 ± 8.44^{a}	26.28 ± 8.04^{a}
	Xylem traits	Vessel density, VD (no./mm^2)	12.48 ± 4.81^{a}	14.6 ± 4.39^{a}	15.24 ± 5.06^{a}
		Vessel area, VA (μm^2)	3406 ± 996^{a}	2855 ± 670^{b}	2882 ± 656^{b}
		Vessel diameter, *D* (μm)	65 ± 10^{a}	60 ± 7^{a}	60 ± 7^{a}
		Hydraulic vessel diameter, D_H (μm)	80.51 ± 11.01^{a}	75.24 ± 9.47^{ab}	70.86 ± 10.08^{b}
		Grouping index (GI)	1.75 ± 0.27^{a}	1.91 ± 0.3^{a}	1.76 ± 0.25^{a}
		Proportion of water-conducting vessel area (*F*)	0.04 ± 0.01^{a}	0.04 ± 0.01^{a}	0.04 ± 0.01^{a}
		Vessel composition index (*S*)	0.03 ± 0.02^{a}	0.02 ± 0.01^{b}	0.02 ± 0.01^{b}
X. moluccensis	Tree characteristics	Sample trees (N)	18	18	11
		Diameter at breast height, DBH (cm)	21.47 ± 9.13^{a}	23.47 ± 4.83^{a}	19.67 ± 5.02^{a}
		Tree height (m)	8.21 ± 2.71^{a}	7.68 ± 1.92^{ab}	6.13 ± 1.22^{b}
		Leaf area, LA (cm^2)	37.56 ± 12.39^{a}	32.52 ± 10.27^{a}	32.32 ± 9.96^{a}
	Xylem traits	Vessel density, VD (no./mm^2)	17.56 ± 3.85^{b}	19.89 ± 4.23^{b}	24.27 ± 3.6^{a}
		Vessel area, VA (μm^2)	5890 ± 897^{a}	5214 ± 1128^{ab}	4787 ± 759^{b}
		Vessel diameter, *D* (μm)	86 ± 7^{a}	81 ± 9^{a}	78 ± 7^{b}
		Hydraulic vessel diameter, D_H (μm)	101.2 ± 8.14^{a}	95.04 ± 10.47^{a}	85.99 ± 9.57^{b}
		Grouping index (GI)	1.54 ± 0.16^{a}	1.58 ± 0.13^{a}	1.49 ± 0.16^{a}
		Proportion of water-conducting vessel area (*F*)	0.1 ± 0.03^{a}	0.1 ± 0.02^{a}	0.11 ± 0.01^{a}
		Vessel composition index (*S*)	0.04 ± 0.01^{a}	0.03 ± 0.02^{a}	0.02 ± 0.01^{a}
H. fomes	Tree characteristics	Sample trees (N)	34	25	7
		Diameter at breast height, DBH (cm)	16.48 ± 5.35^{a}	15.07 ± 4.37^{a}	14.64 ± 3.71^{a}
		Tree height (m)	9.03 ± 3.06^{ab}	10.39 ± 4.37^{a}	10.2 ± 2.19^{b}
		Leaf area, LA (cm^2)	41.63 ± 13.05^{a}	39.29 ± 11.73^{a}	42.08 ± 9.45^{a}
	Xylem traits	Vessel density, VD (no./mm^2)	7.56 ± 1.87^{c}	9.68 ± 4.2^{b}	9 ± 3.95^{a}
		Vessel area, VA (μm^2)	8455 ± 2784^{a}	7450 ± 2173^{ab}	6536 ± 2660^{b}
		Vessel diameter, *D* (μm)	102 ± 17^{a}	96 ± 14^{a}	79 ± 12^{b}
		Hydraulic vessel diameter, D_H (μm)	135.78 ± 22.99^{a}	127.62 ± 21.05^{a}	108.43 ± 8.97^{b}
		Grouping index (GI)	1.58 ± 0.16^{b}	1.67 ± 0.2^{ab}	1.52 ± 0.35^{a}
		Proportion of water-conducting vessel area (*F*)	0.06 ± 0.02^{a}	0.07 ± 0.01^{a}	0.05 ± 0.02^{a}
		Vessel composition index (*S*)	0.12 ± 0.06^{a}	0.1 ± 0.06^{ab}	0.06 ± 0.02^{b}

Note: Different letters denote statistically significant ($p < 0.05$).

Abbreviation: SD, standard deviation.

3.2 | Phylogenetic relationships

The analyses of phylogenetic signals across various xylem and hydraulic traits revealed a range of Blomberg's *K*-values, reflecting varying degrees of phylogenetic effects. Traits, such as VA ($K = 6.37$), *D* ($K = 6.05$), D_H ($K = 5.39$), *S* ($K = 5.38$), *F* ($K = 4.05$) and VD ($K = 3.76$), exhibited the strongest phylogenetic signals. Compared with most of the xylem traits, hydraulic traits, such as K_P ($K = 2.35$), K_L ($K = 2.31$) and $(t/b)^2$ ($K = 1.18$), exhibited a lower phylogenetic effect. These *K*-values were statistically significant ($p = 0.001$) based on 1000 randomizations. However, GI ($K = 0.97$) had a weak (*K*-value <1) phylogenetic signal. The correlations derived from PICs were consistent with species-wise correlations (Table 2), indicating that the observed relationships among the traits were largely independent of phylogenetic relatedness.

3.3 | Association between xylem and hydraulic traits

Increasing *S* and *F* in the studied species resulted in significant increases in K_P and K_L (Table 2, $p < 0.05$). Similarly, *D*, D_H and VA increased significantly with both K_P and K_L but inversely with VD. As

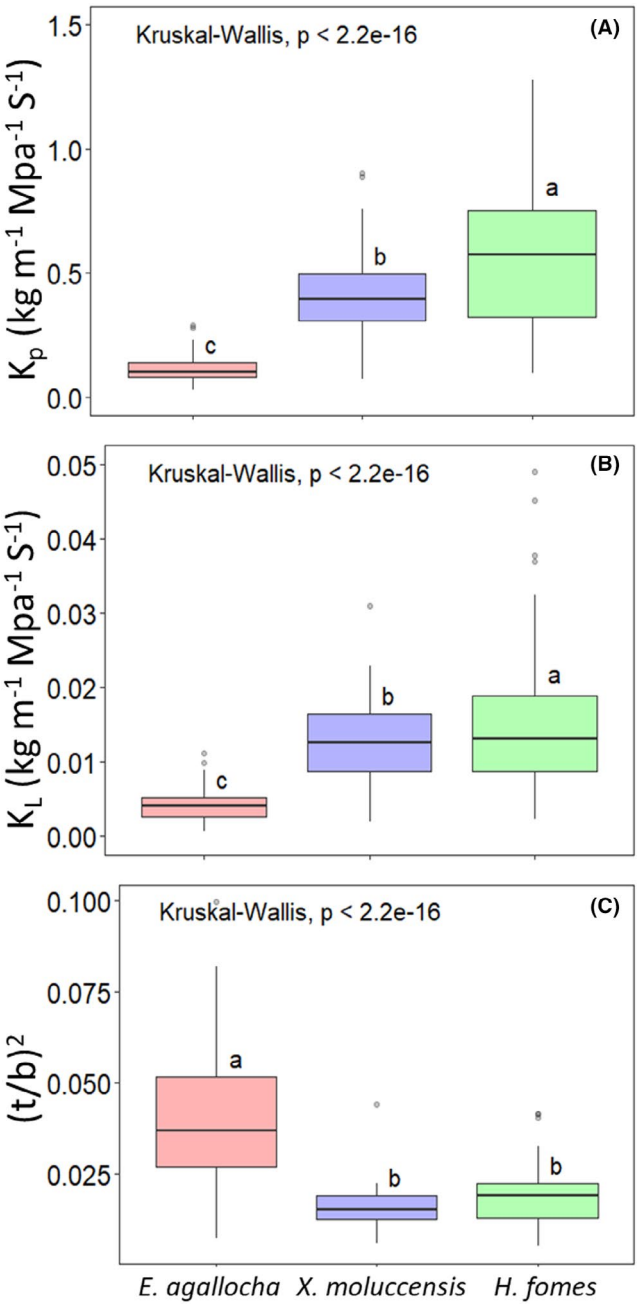


FIGURE 3 Hydraulic traits variation among the species in the Bangladesh Sundarbans. K_p, Potential conductivity (A); K_L, Leaf-specific conductivity (B); $(t/b)^2$, vessel wall reinforcement (C). Different letters denote statistically significant variation at $p < 0.05$ and same letters are not significant ($p < 0.05$).

a result, increasing VD significantly reduced *D*, D_H and VA. On the contrary, K_p and K_L showed no significant decreasing trend when $(t/b)^2$ increased. However, the correlations between K_p or K_L and GI were negative and statistically significant ($p < 0.05$).

The PCA provided insights into the trade-offs between hydraulic conductance and hydraulic resistance, and their structural underpinnings across salinity gradients (Figure 4). The biplot revealed two significant principal components that accounted for 80.1% of the variability among the samples. The first component (PC1) explained 59.3% of the variation in the dataset and exhibited strong positive loadings with K_p, K_L, *D*, D_H and *S* but negative loadings with $(t/b)^2$ and GI. The second component (PC2) explained 20.8% of the variation and was strongly related to VD and *F*. The individual trait and the salinity zone exhibited a distinct pattern in the biplot (Figure 4). For example, the LSZ was aligned mainly with PC1. On the contrast, the MSZ and the HSZ were distributed mainly in the opposite direction of PC1. In addition, fewer MSZ and HSZ data were aligned with PC2.

3.4 | Vessel diameter variation among the species

Although vessel diameter (*D*) exhibited a unimodal distribution, the patterns varied among the species. For example, most of the vessels were wider and had a right-skewed distribution in *H. fomes* (Figure 5A); conversely, most of the narrow diameter vessels in *E. agallocha* had a left-skewed distribution. The *D* also varied significantly among the study species, where the highest *D* was found in *H. fomes* and the lowest in *E. agallocha* (Figure 5B).

3.5 | Effects of habitat variables on vessel diameter

Habitat variables, such as regulators (soil salinity, siltation, pH and elevation), resources (NH_4, P and K) and forest structural variables (tree density, tree height, CoV DBH and CoV height), moderately explained the variability in vessel diameter (*D*) across the study species (Table 3). The models exhibited interactive effects of the habitat variables on *D* (model confidence set, ΔAIC ≤2). Among the regulatory variables, soil salinity had a relatively strong negative effect on *D* (Figure 6, Table 3). The pH and silt percentage had positive influences on *D* in *X. moluccensis*. However, increasing elevation gradually decreased *D* in *H. fomes*.

Although NH_4 had a positive influence on *D* in *E. agallocha*, it decreased to ~6 mg^{-1} NH_4 and then increased gradually in *X. moluccensis* (Figure 6). On the contrary, *D* had a negative trend after a gradual increase of P to ~30–40 mg^{-1} in *E. agallocha* and *X. moluccensis*. The *D* increased to ~5–6 mg^{-1} *K* in *E. agallocha* and *X. moluccensis*, and then decreased with increasing *K*. On the contrary, *D* showed a negative trend with increasing *K* in *H. fomes*.

Among the forest structural variables, tree height and DBH had positive influences on *D* in *E. agallocha* and *X. moluccensis* (Figure 6). In the case of *H. fomes*, both variables increased *D* up to ~10 m in height and ~20 cm in DBH and then showed an almost constant trend. Although *D* increased with increasing CoV height in *X. moluccensis*, a constant variation was found after an increase in *D* of ~20% of the CoV height in *H. fomes*. The CoV DBH gradually increased *D* in *H. fomes* and *X. moluccensis*. In *E. agallocha*, *D* variation was constant reaching ~25% of the CoV DBH, and subsequently increased. Tree density had a positive influence on *D* up to a certain tree density in the plots (~350 ha^{-1}) and then exhibited a decreasing trend in *H. fomes* and *X. moluccensis* (Figure 6).

TABLE 2 Correlations between traits in the studied tree species in the Sundarbans.

Variables	*F*	*S*	$(t/b)^2$	K_P	K_L	GI	VD	D_H	*D*	VA
F		0.135	−0.146	**0.683**	**0.654**	**−0.297**	**0.405**	**0.404**	**0.582**	**0.568**
S	0.155		**−0.576**	**0.611**	**0.539**	**−0.322**	**−0.851**	**0.857**	**0.884**	**0.878**
$(t/b)^2$	−0.089	**−0.621**		−0.140	−0.155	**0.416**	**0.224**	**−0.625**	**−0.747**	**−0.726**
K_P	**0.544**	**0.150**	−0.091		**0.922**	**−0.277**	−0.102	**0.917**	**0.823**	**0.834**
K_L	**0.330**	**0.368**	−0.151	**0.834**		**−0.215**	−0.151	**0.830**	**0.751**	**0.764**
GI	**−0.188**	**−0.220**	**0.215**	**−0.179**	**−0.164**		0.140	**−0.288**	**−0.404**	**−0.393**
VD	**0.570**	**−0.904**	**0.378**	−0.110	−0.126	**0.165**		**−0.577**	**−0.507**	**−0.509**
D_H	**0.223**	**0.584**	**−0.320**	**0.872**	**0.853**	**−0.168**	**−0.390**		**0.894**	**0.903**
D	**0.338**	**0.872**	**−0.636**	**0.413**	**0.515**	**−0.227**	**−0.580**	**0.668**		**0.988**
VA	**0.334**	**0.869**	**−0.628**	**0.417**	**0.518**	**−0.212**	**−0.579**	**0.671**	**0.995**	

Note: Species-wise correlations are shown above and phylogenetically independent contrast (PIC) correlations below the diagonal. Significance levels: bold $p < 0.05$. All data were log-transformed.

Abbreviations: *D*, vessel diameter; D_H, hydraulically weighted vessel diameter; *F*, proportion of water-conducting vessel area; GI, grouping index; K_L, leaf-specific conductivity; K_P, potential conductivity; *S*, vessel composition index; $(t/b)^2$, vessel wall reinforcement; VA, vessel area; VD, vessel density.

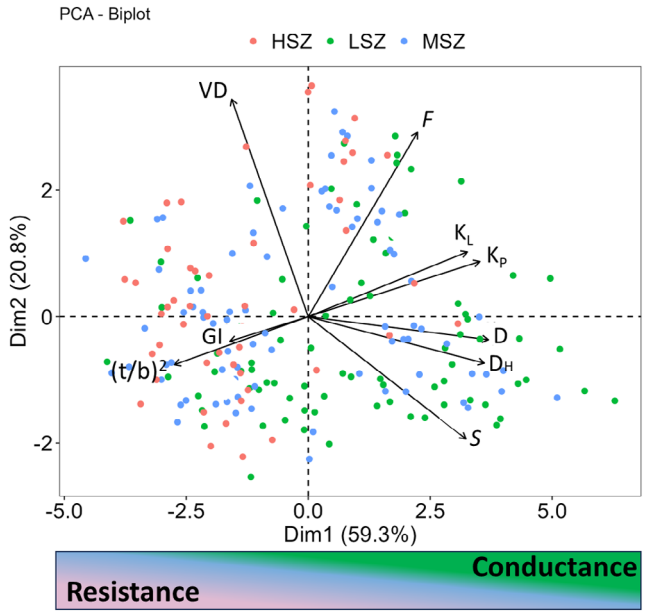


FIGURE 4 Principal components analysis (PCA) depicting the two significant principal components and the relationships among hydraulic (K_P, potential conductivity; K_L, leaf-specific conductivity; $(t/b)^2$, vessel wall reinforcement) and xylem traits (*D*, vessel diameter; D_H, hydraulically weighted vessel diameter; *S*, vessel composition index; *F*, proportion of water-conducting vessel area; VD, vessel density; GI, grouping index) in the study species. The salinity zones in the Sundarbans, that is the low (LSZ), the medium (MSZ) and the high (HSZ) salinity zone.

4 | DISCUSSION

4.1 | Species-specific hydraulic strategies along salinity gradients

We investigated how xylem and hydraulic traits vary among the studied mangrove species growing in climatically identical but distinct salinity zones (the LSZ, MSZ and HSZ) in the Sundarbans. As predicted, the studied species showed decreased potential conductivity (K_P) and leaf-specific conductivity (K_L) values from the LSZ to the HSZ (Figure 2). However, the K_P variation among the salinity zones was significant for *E. agallocha* and *H. fomes*. A higher salinity at the HSZ could reduce the conductive area and consequently decrease hydraulic conductivity. Vessel diameter (*D*) decreased significantly from the LSZ to the HSZ, whereas VD increased with increasing salinity (Table 1). These findings are consistent with earlier studies on other mangrove species, such as *Rhizophora mucronata* Lamk., *A. germinans* (L.) in Kenya, Australia and Florida (Lovelock et al., 2006; Madrid et al., 2014; Robert et al., 2009; Schmitz et al., 2006). On the contrary, K_L varied significantly across the salinity gradients only in *H. fomes* (Figure 2). The nonsignificant variation in K_L among the salinity zones in *E. agallocha* and *X. moluccensis* (Table 1) might be due to a gradual decrease in leaf area as salinity increased. Furthermore, other mechanisms, such as increased water storage, reduced leaf area and leaf thickness, may help to adapt at relatively high salinities, as described for other mangrove species (Jiang et al., 2017; Nguyen et al., 2017).

The vessel composition index (*S*) was significantly higher at the LSZ in the study species, except for *X. moluccensis* (Table 1). A relatively low *S* in the higher salinity zone indicates a more hydraulically conservative strategy with many small vessels and a potentially lower risk of salinity-induced embolism (Carlquist, 2016, 2018; Schenk et al., 2008; Tyree, 2003; Zanne et al., 2010). On the contrary, *F* did not differ significantly among the salinity zones (Table 1). The mean *F* values for the study species (Table 1) are within the range reported for angiosperms (<0.20; Jacobsen et al., 2007). However, the vessel GI significantly varied among the salinity zones only in *H. fomes* (Table 1). Different types of wood construction have different vessel porosities, indicating the influence of zone- and species-specific mechanical support requirements (McCulloh et al., 2004; McCulloh & Sperry, 2005;

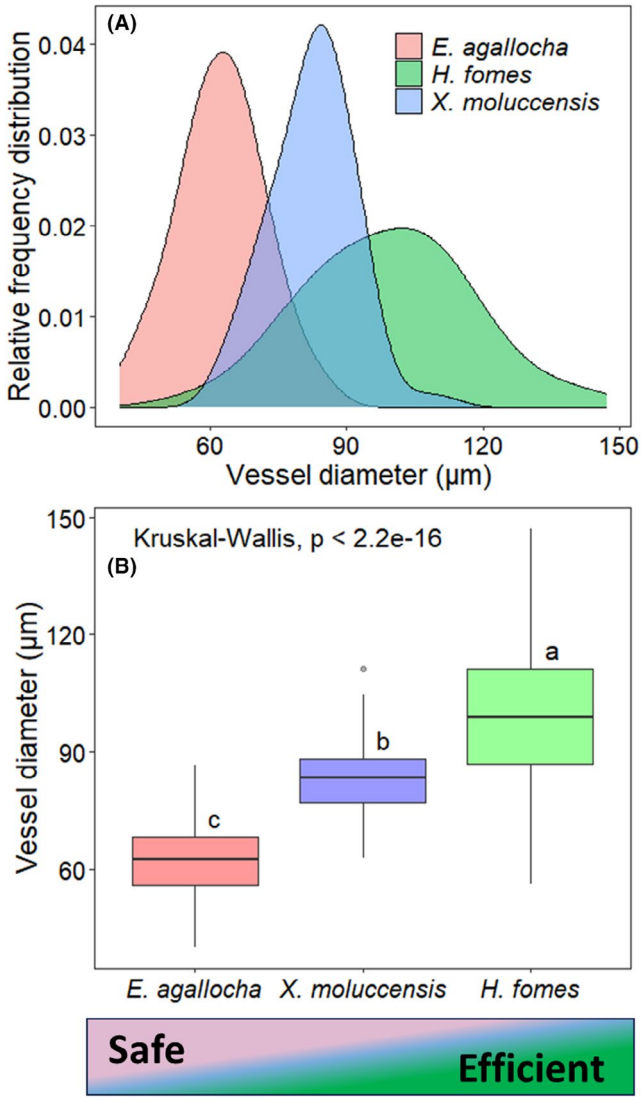


FIGURE 5 Frequency distribution of the vessel diameters (A) and the mean vessel diameter variation (B) among the studied species. Different letters denote statistically significant variation at $p < 0.05$.

Zanne et al., 2010). Additionally, increases in the total amount of vessel lumens might lead to greater intervessel connectivity (Mrad et al., 2021; Pratt et al., 2007; Venturas et al., 2019). Higher intervessel connectivity is advantageous in trees, especially in higher salinity areas, because water may bypass alternative pathways formed by the intervessel pits of neighbouring vessels, if any vessel is cavitated (Baas et al., 1983; López-Portillo et al., 2005; Yáñez-Espinosa et al., 2001; Zimmermann, 2002).

As assumed, vessel wall reinforcement $(t/b)^2$ increased from the LSZ to the HSZ in the study species (Figure 1). The $(t/b)^2$ value was significantly lower in the LSZ than in the MSZ and the HSZ; however, the difference was not significant between the MSZ and the HSZ (Table 1). A relatively high $(t/b)^2$ has therefore evolved into a strategy to cope with salinity stress at relatively high salinities. The intraspecific plasticity of xylem structures related to hydraulic functioning across salinity gradients is beneficial because changing embolism resistance contributes to salinity tolerance (Robert et al., 2009). The observed zone-specific hydraulic traits in high- to low-salinity environments may reflect species differences in water use and salinity tolerance strategies in the Sundarbans.

4.2 | Phylogenetic constraints on the relationships between xylem and hydraulic traits

The observed phylogenetic signals across various xylem and hydraulic traits in our study species highlight phylogenetic constraints in hydraulic strategies. We observed that xylem traits, such as VA, D and D_H, had greater phylogenetic conservatism, suggesting that these characteristics are conserved among closely related species in mangroves. However, the phylogenetic signal was comparatively lower for hydraulic traits, such as K_P and K_L, which thus appears to be less constrained by evolution than vessel size and number. The K_P or K_L values can be modulated by a combination of vessel size, and a small change in VA has a large effect on hydraulic conductivity. These findings are in agreement with the findings of Carlquist and Hoekman (1985), who reported that VD changes more rapidly than vessel size. Our results suggest that traits related to hydraulic efficiency and safety are conserved phylogenetically, implying that the studied species are functionally similar except for GI, possibly as a result of ecological niche conservatism, as described in earlier studies (Carvalho et al., 2023; Liu et al., 2015; Webb et al., 2002). Despite these constraints, the correlations derived from PICs in our study (Table 2) indicate that the relationships between xylem and hydraulic traits are not regulated by phylogenetic relatedness.

4.3 | Hydraulic strategies in relation to the shade tolerance of species

Earlier studies (Lohbeck et al., 2013; Poorter et al., 2018) reported that light-demanding species tend to have high photosynthetic rates to maximize carbon gain and thus tree growth. Owing to its relatively high growth rate, light-demanding *E. agallocha* (Chowdhury, De Ridder, & Beeckman, 2016; Chowdhury, Sarker, Sultana, et al., 2023; Siddique et al., 2021) might require a greater hydraulic supply than comparatively slow-growing shade-bearing *H. fomes* to sustain carbon assimilation. Contrary to expectations, the K_P and K_L values were significantly lower in light-demanding *E. agallocha* than in both shade-tolerant species in the Sundarbans (Figure 3A,B). Although there was a significant negative correlation between D and VD, VA had a greater effect on the K_P and K_L than did VD (Table 2). Wide vessels result in high flow rates for a given pressure gradient (Kondoh et al., 2006). Higher hydraulic conductivity increases stomatal conductance and photosynthetic rates (Guyot et al., 2012; Meinzer et al., 2010). Therefore, shade-tolerant *X. moluccensis* and *H. fomes* with few large vessels have higher conductivity than light-demanding *E. agallocha* with many small vessels. In addition to having lower K_P and K_L values

TABLE 3 Results of generalized additive models (GAMs) built to determine the vessel diameter variation to multiple habitat variables in the Sundarbans.

Species	Model rank	Habitat variables												ΔAICc	AICcw	DE%	Adj.R^2
		Salinity	Silt	pH	Elevation	NH_4	P	K	Height	DBH	CoV height	CoV DBH	Tree density				
E. agallocha	1	+	+	−	−	+	+	+	−	+	−	+	+	0	0.2	53	0.38
	2	+	+	−	−	+	+	+	−	+	+	+	−	0.4	0.2		
	3	+	+	−	−	+	+	+	−	+	+	+	+	0.7	0.2		
	4	+	+	−	−	+	+	+	−	+	−	−	+	1.1	0.1		
	5	+	+	−	−	+	+	−	−	+	−	+	+	1.5	0.1		
	RI	0.9	0.6	0.3	0	0.5	0.9	0.6	0.4	0.72	0.5	0.7	0.5				
X. moluccensis	1	+	+	+	−	+	+	+	−	+	+	−	−	0	0.3	67	0.47
	2	+	−	+	−	+	−	−	+	−	+	+	+	1.4	0.2		
	3	−	+	+	−	−	−	−	+	+	+	+	+	1.7	0.1		
	4	−	+	+	−	+	+	+	−	+	+	+	−	1.8	0.1		
	5	+	+	+	−	+	+	+	−	−	+	−	−	1.9	0.1		
	RI	0.6	0.6	0.9	0	0.8	0.4	0.4	0.8	0.51	0.7	0.5	0.6				
H. fomes	1	+	−	−	+	−	+	+	−	+	−	−	+	0	0.3	61	0.42
	2	+	−	−	+	−	+	+	−	+	+		+	1.3	0.2		
	3	+	−	−	+	−	+	+	−	+		+	+	1.4	0.1		
	4	+	−	−	−	−	+	+	+	+	−	−	+	1.4	0.1		
	5	−	−	−	+	−	+	+	−	+	−	−	+	1.5	0.1		
	RI	0.7	0.3	0.3	0.7	0.3	0.9	0.7	0.3	0.9	0.3	0.4	0.9				

Note: DE (%), deviance explained (%); RI, relative importance of the variable in the model selection process; ΔAICc, the difference between the AICc value of the best model and the AICc values of the other models; Akaike weights (AICcw), the relative likelihood of each model being the best model in the given data. Positive (+) signs highlight covariates that were retained in the best model. Dash indicates no participation of that covariate in any of the candidate models. The covariates are: soil salinity (electrical conductivity; EC, $mS\,cm^{-1}$), elevation (m, above msl), silt (%), NH_4 ($mg\,g^{-1}$), P ($mg\,g^{-1}$), K ($mg\,g^{-1}$), height (m), DBH (cm), (coefficient of variation) CoV of height, CoV of DBH and tree density (no. ha^{-1}).

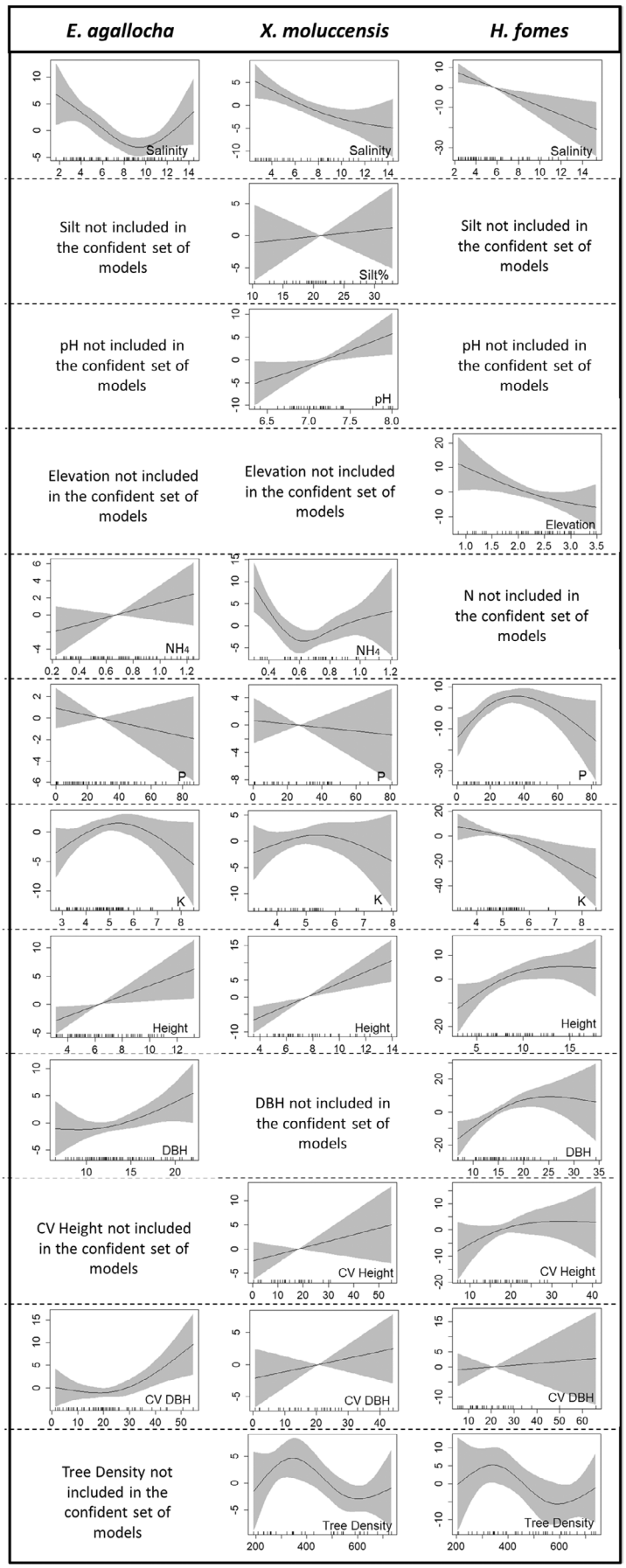


FIGURE 6 Habitat influences inferred from the best generalized additive models (GAM) fitted to the vessel diameter in the study species in the Sundarbans. The solid line in each plot is the estimated spline function (on the scale of the linear predictor) and shaded areas represent the 95% confidence intervals. The negative values on the *y*-axis relate to vessel diameter reductions and positive values relate to diameter increases in GAM. Zero on the *y*-axis indicates no effect of the variable on vessel diameter (given that the other variables are included in the model). Soil salinity (electrical conductivity, EC, $mS\,cm^{-1}$), elevation (m, above m.s.l.), silt (%), NH_4 ($mg\,g^{-1}$), P ($mg\,g^{-1}$), K ($mg\,g^{-1}$), height (m), DBH (cm), CoV (coefficient of variation) of height, CoV (coefficient of variation) of DBH and tree density (no. ha^{-1}).

(Figure 3A,B), a greater growth rate in light-demanding than in both shade-tolerant species (Rahman et al., 2020; Siddique et al., 2021) suggests a comparatively higher water use efficiency (WUE) and lower transpiration loss in *E. agallocha*.

We expect that shade-tolerant species have high hydraulic safety but suffer from low hydraulic efficiency, and this trade-off enhances the ability of trees to grow in stressed conditions, such as those in high salinity and/or shaded habitats (Markesteijn et al., 2011). In contrast to the prediction, light-demanding *E. agallocha* had significantly greater $(t/b)^2$ values but lower K_P and K_L values than the studied shade-tolerant species (Figure 3C). Furthermore, a nonsignificant inverse correlation between K_P or K_L and $(t/b)^2$ (Table 2) suggests a weak hydraulic safety–efficiency trade-off in the studied mangrove species irrespective of the shade tolerance of the species. Similarly, earlier studies (Jiang et al., 2017, 2021) reported a lack of a trade-off between hydraulic safety and efficiency in other mangrove species (e.g. *A. marina* (Forssk.) Vierh., *Aegiceras corniculatum* (L.) Blanco, *Bruguiera gymnorrhiza* (L.) Lam., *Kandelia obovate* (L.) Druce, *Hibiscus tiliaceus* (L.) and *Pongamia pinnata* (L.) Pierre) regardless of shade tolerance ability. Similarly, global interspecific analysis revealed a weak trade-off between hydraulic safety and efficiency in diverse plant species (Gleason et al., 2016; Liu et al., 2021). Although a higher vessel grouping increases hydraulic safety (Carlquist, 2009; von Arx et al., 2013), a significant negative correlation between GI and K_P or K_L (Table 2) indicates that GI reduces hydraulic conductivity. This hydraulic flow reduction is compensated by increasing *D* (owing to a significant positive correlation with K_P and K_L; Table 2), as described by Lens et al. (2011) and Okello et al. (2017). We therefore infer that the studied mangrove species could adapt to hydraulic limitations and shade conditions by changing their xylem structures.

4.4 | Vessel diameter determines a safe hydraulic system

According to the PCA (Figure 4), vessel diameters across the salinity zones were strongly related to the variations in K_P and K_L. We also found that *S* (the proportion of higher diameter vessels) and *F* (the cross-sectional space occupied by vessel lumens) were coupled with hydraulic conductivity. This was likely due to the influence of many wider vessels with low vessel interconnectivity. In contrast, the tendency to form group vessels in mangrove species might be interpreted as a safe mechanism against embolism since a greater percentage of vessels remain functional through greater vessel interconnectivity, whereas some vessels are cavitated (Baas et al., 1983; Jacobsen & Pratt, 2023; Mauseth & Plemons-Rodriguez, 1998; Mrad et al., 2021; Robert et al., 2009; Schmitz et al., 2006). The first component can therefore be interpreted as a trade-off between conductance efficiency (indicated by K_P, K_L, *D* and *S*), which is more emphasized in the LSZ, and hydraulic resistance, as reflected by $(t/b)^2$, GI and VD, is prominent both in the HSZ and the MSZ (Figure 4).

Based on the different D distributions (Figure 5A), it can be inferred that the hydraulic transport systems are highly different among the study species. For example, light-demanding *E. agallocha* had a left-skewed vessel distribution where most of the vessels were narrow. On the contrary, shade-tolerant *H. fomes* had a right-skewed D distribution with mostly wider vessels. Another shade-tolerant species, *X. moluccensis*, had a vessel distribution between those of *E. agallocha* and *H. fomes*, where vessels of intermediate size were more common. Furthermore, the decrease in *D* from right to left-skewed species across salinity gradients indicates a lower conductive efficiency, which is related to increased conductive safety (Figure 5A), as described in other mangroves (Robert et al., 2009). *E. agallocha* had not only a smaller *D* (Figure 5B) than the two other study species did but also a greater proportion of the tiniest vessels. Earlier studies (Carlquist, 2016, 2018; Jacobsen & Pratt, 2023; Lens et al., 2023) reported that narrow vessels are positively related to low vulnerability to cavitation, which indicates that the hydraulic transport system of light-demanding *E. agallocha* is relatively safer than those of two other shade-tolerant species. Although the phenotypic plasticity of xylem traits is different from the mechanistic understanding (Jiang et al., 2022), the divergent vessel structures of coexisting study species in the Sundarbans might have a major influence on salinity tolerance and, subsequently, on their distribution across the ecosystem.

4.5 | Habitat influences on vessel diameter variation

Among the xylem traits, *D* is an important trait that strongly influences hydraulic efficiency and safety (Figures 4 and 5); thus, we explored the influences of habitat variables on *D* variation (Figure 6). Among the GAMs, regulators, resources and forest structure moderately explained *D* variability (deviation explained, 62.8%; Table 3). Among the regulatory variables, soil salinity had a strong negative influence on *D* in *H. fomes* and *X. moluccensis* (Figure 6). Conversely, the soil salinity decreased *D* up to ~10 $mS\,cm^{-1}$ in *E. agallocha*; afterwards, it almost plateaued with increasing salinity. As *D* was positively correlated with K_P and K_L (Table 3), reducing *D* might limit photosynthetic carbon gain in trees (Chen & Ye, 2014; Lovelock et al., 2006). However, *E. agallocha* may increase the capacity for photosynthetic carbon gain under high salinity conditions, providing this species a competitive advantage under more saline conditions. The silt percentage had little influence on *D* variation (Figure 6). Earlier studies (De Deurwaerder et al., 2016; Okello et al., 2017) demonstrated that siltation reduces vessel size in *A. marina* and *Rhizophora mucronata*. Siltation may develop stress due to the burying root system, causing trees to reduce vessel size. Mangrove trees can minimize such stress by developing pneumatophores or knee roots (Hossain, 2015), resulting in a lower influence on *D* variability. Although *D* in *E. agallocha* and *H. fomes* was not sensitive to pH, a positive influence was found in *X. moluccensis* (Figure 6). This indicates a lower influence of soil pH on hydraulic transport and thus tree

growth in the Sundarbans (Chowdhury, Sarker, Sultana, et al., 2023; Sarker et al., 2021). However, elevation had a negative influence on *D* only in *H. fomes*. The elevated areas receive less inundated water in the Sundarbans, which may create hydraulic stress, as described in Kenyan mangroves (De Deurwaerder et al., 2016).

Although nutrient availability among the study zones might have interfered with salinity in the Sundarbans (Ahmed, Sarker, Friess, et al., 2023), the hydraulic conductivity of tree species is expected to vary in response to nutrient variability (Arnold & Mauseth, 1999). Nutrient availability can influence cell formation and induce changes in vessel size and arrangement (Hacke, 2015; Tyree & Zimmermann, 2002). Among the study species, *D* was slightly sensitive to NH_4 in *E. agallocha* (Figure 6). An earlier study of Lovelock et al. (2006) reported that at N-limited sites, fertilization with N stimulated growth in other mangrove species (*A. germinans*, *R. mangle* and *L. racemosa*) without affecting hydraulic conductivity. On the contrary, P increased *D* up to 20–30 mg^{-1} in the study species, and then exhibited a decreasing trend (Figure 6). However, the effect was lower in *X. moluccensis* than in the other two species (Table 3). The increase in hydraulic conductivity resulting from the availability of P was associated with increased *D* in Florida, Panama and Belizean mangroves (Lovelock et al., 2004, 2006). Similarly, *K* increased the vessel diameter up to 5–6 mg^{-1}, and then decreased with increasing *K* (Figure 6). A decrease in K^+ absorption induced by osmotic stress (Lintunen et al., 2017) could lead to a decrease in D and thus hydraulic conductivity in mangroves.

Forest structural variables, such as tree height, DBH and tree density, increase resource (e.g. light and nutrients) heterogeneity and competition, which influence tree growth and distribution in the Sundarbans (Ahmed, Sarker, Kamruzzaman, et al., 2023; Chowdhury, Sarker, Sultana, et al., 2023; Sarker et al., 2019) and are thus expected to influence hydraulic functioning in trees. Among them, tree height increased *D* in each case (Figure 6). A wider *D* allows a greater hydraulic supply within the same leaf area over a longer distance in taller trees. A higher conductivity might help them compensate for longer pathways and concomitant hydraulic resistance by adjusting their vessel anatomy, as described for trees in other ecosystems (Bittencourt et al., 2022; Olson et al., 2014; Sperry et al., 2008). Compared with *X. moluccensis*, DBH had a greater positive influence on *D* in *E. agallocha* and *H. fomes* (Figure 6). Larger trees might have exposed crowns and therefore need high hydraulic conductivity and associated traits to meet their high transpiration requirements. At the community level, tree size inequality results from both inter- and intraspecific differences in height and DBH, which may enhance the efficient use of resources (e.g. light) for growth (Zhang & Chen, 2015). As assumed, tree size inequality (CoV height and CoV DBH) had positive influences on *D*, although the patterns of variation varied among the study species (Figure 6). Higher forest structural diversity allows higher tree densities at different tree canopy heights and increases light availability, which could increase potential productivity (Parker et al., 2004; Yachi & Loreau, 2007; Zhang & Chen, 2015). The *D* increased up to a certain tree density up to the tree density (350 no. ha^{-1}) in *H. fomes* and *X. moluccensis* and then decreased with increasing tree density. As shade bearers, both species prefer diffuse light for growth, which might be available up to a certain tree density. An increase in *D* enables trees with higher conductivity to enhance carbon gain (Lovelock et al., 2006). In higher canopy gaps, shade bearers cannot effectively utilize light resources for carbon gain, thereby decreasing vessel diameters to minimize hydraulic costs.

4.6 | Implications

In addition to other consequences (such as increases in temperature, variability in the seasonality of precipitation and frequent storm events) of climate change (Zaman et al., 2017), the Bangladesh coast is highly vulnerable to SLR (Kanan et al., 2023). Although the Sundarbans is a sea-dominated active delta, the river network regulates salinity within the ecosystem through the influx of upstream river flows. In addition to salinity intrusion from the sea, historical decreases in freshwater flows in the main distributary river due to damming increase the salinity in the ecosystem (Bricheno et al., 2021). Furthermore, the relatively high sedimentation rate (~2.4 billion tons of sediments $year^{-1}$; Mitra & Zaman, 2016) on this coast also affects the degree of siltation in the Sundarbans. Therefore, increasing salinity and higher siltation increase stress on trees, which affects species survival/growth–salinity coupling, resulting in local extinction or range contraction (towards low-salinity areas) of species, particularly the globally endangered *H. fomes* in the Sundarbans (Chowdhury, Sarker, Sultana, et al., 2023; Sarker et al., 2016, 2019). The Bangladesh government has been planning to protect and conserve the Sundarbans through different global mechanisms of climate change mitigation, such as 'reducing emissions from deforestation and forest degradation (REDD+)' (Ahmed & Glaser, 2016). In this context, a baseline assessment of the hydraulic characteristics of mangrove species that incorporates hydraulic characteristics in the species selection process would help in the design of climate-smart mangrove restoration programmes. For example, we showed that the hydraulic structure of *E. agallocha* is safer than that of *H. fomes*, followed by *X. moluccensis* (Figure 5). The contrasting ecological distributions of the study species in the Sundarbans (Sarker et al., 2016, 2019) are reflected at least partially by their divergent hydraulic characteristics. Species-specific hydraulic design might also help to predict species distributions in the Sundarbans, particularly in relation to salinity.

In addition, other xylem traits, such as cell fractions, vessel length, cell ultrastructure, pit membrane and perforation plate, and their interactions, could be used to understand the specific-specific hydraulic safety–efficiency relationships in mangroves (Choat et al., 2007; Jacobsen et al., 2012; Plavcová & Hacke, 2012; Schmitz et al., 2012b). Future investigations should focus on the integration of these traits as a potential avenue to refine hydraulic distinctiveness across plant functional groups in response to environmental changes.

5 | CONCLUSIONS

This study, for the first time, analysed the variation in xylem traits, such as VD, vessel diameter (*D*) and vessel GI, and hydraulic traits, such as potential conductivity (K_P), leaf-specific conductivity (K_L) and vessel wall reinforcement $(t/b)^2$, in three dominant tree species across salinity gradients in the Sundarbans. The results revealed that across the study species and salinity gradients, the K_P and K_L values in the studied species were constrained mainly by salinity. On the contrary, the study species exhibited a greater $(t/b)^2$ in response to high salinity. Although all xylem traits except GI had strong phylogenetic signals, vessel traits, such as *D* and VD evolved in a coordinated way, suggesting that the species are flexible in terms of hydraulic adjustment. Among the species, the shade-tolerant *H. fomes* and *X. moluccensis* had significantly greater K_P and K_L values than did the light-demanding *E. agallocha*. Although we found a weak trade-off between hydraulic safety and efficiency in the xylem, the variation in *D* indicates that the water transport systems are highly different among the species. Compared with that of *H. fomes*, the hydraulic design of *E. agallocha* is safer but less efficient, followed by that of *X. moluccensis*. In the future, increasing environmental stress, particularly salinity, in the Sundarbans region will lead to hydraulic failure of the most dominant *H. fomes*. Future studies should focus on integrating other methods for characterizing embolism spread for mechanistic understanding, such as the pneumatic method (Bittencourt et al., 2018; Brum et al., 2023), and characterizing other xylem traits, such as the distribution of cell fractions and pit structure, to improve our understanding of the relationship between hydraulic structures and hydraulic functioning in the Sundarbans. However, understanding the combined influences of habitat (regulators, nutrients and forest structure) variables on hydraulic design across a broad range of salinities provides new insights into the processes underlying hydraulic constraints and will improve our ability to predict how mangroves could be impacted by future environmental changes.

AUTHOR CONTRIBUTIONS

Qumruzzaman Chowdhury and Hans Beeckman conceived the study and designed the experiment. Qumruzzaman Chowdhury and Swapan Kumar Sarker collected the samples. Qumruzzaman Chowdhury, Swapan Kumar Sarker, Anup Datta, Syeda Kaifee Akhter and Zubayer Ahmed analysed the samples. Imam Hossain Imran analysed the data. Qumruzzaman Chowdhury led the writing of the manuscript. All authors provided critical feedback on earlier drafts, contributed substantially to the final version of the manuscript and gave final approval for publication.

ACKNOWLEDGEMENTS

We sincerely acknowledge and thank the Bangladesh Forest Department for the permission (BFD-22.01.0000.004.04.21.1.20.588) and providing support during the fieldwork. We are also grateful to A.Z.M.M. Rashid, R. Sultana, M.S.R. Saimun, A. Saleh, Tokin, Mamun, Faruque and Anis for their support in the fieldwork. We thank M. Marma and S. Azad for her help in the data compilation. We are thankful to Associate Editor and three anonymous reviewers for their critical reviews, constructive comments and suggestions on the earlier version of the manuscript. We sincerely acknowledge the SUST Research Centre for providing research grants to MQC (Project IDs: FES/2020/1/05; FES/2021/2/03).

CONFLICT OF INTEREST STATEMENT

The authors declare that they have no conflicts of interest.

DATA AVAILABILITY STATEMENT

Data are available from the Dryad Digital Repository: https://doi.org/10.5061/dryad.18931zd74 (Chowdhury, Sarker, Imran, et al., 2025).

ORCID

Md. Qumruzzaman Chowdhury https://orcid.org/0000-0002-1766-1185

REFERENCES

Ahmed, N., & Glaser, M. (2016). Coastal aquaculture, mangrove deforestation and blue carbon emissions: Is REDD+ a solution? *Marine Policy*, *66*, 58–66. https://doi.org/10.1016/j.marpol.2016.01.011

Ahmed, S., Sarker, S. K., Friess, D. A., Kamruzzaman, M., Jacobs, M., Sillanpää, M., Naabeh, C. S. S., & Pretzsch, H. (2023). Mangrove tree growth is size-dependent across a large-scale salinity gradient. *Forest Ecology and Management*, *537*, 120954. https://doi.org/10.1016/j.foreco.2023.120954

Ahmed, S., Sarker, S. K., Kamruzzaman, M., Ema, J. A., Naabeh, C. S. S., Cudjoe, E., Chowdhury, F. I., & Pretzsch, H. (2023). How biotic, abiotic, and functional variables drive belowground soil carbon stocks along stress gradient in the Sundarbans Mangrove Forest? *Journal of Environmental Management*, *337*, 117772. https://doi.org/10.1016/j.jenvman.2023.117772

Arenas-Navarro, M., Oyama, K., García-Oliva, F., Torres-Miranda, A., de la Riva, E. G., & Terrazas, T. (2021). The role of wood anatomical traits in the coexistence of oak species along an environmental gradient. *AoB Plants*, *13*(6), plab066. https://doi.org/10.1093/aobpla/plab066

Arnold, D. H., & Mauseth, J. D. (1999). Effects of environmental factors on development of wood. *American Journal of Botany*, *86*(3), 367–371. https://doi.org/10.2307/2656758

Aziz, A., & Paul, A. R. (2015). Bangladesh Sundarbans: Present status of the environment and biota. *Diversity*, *7*(3), 242–269. https://doi.org/10.3390/d7030242

Baas, P., Werker, E., & Fahn, A. (1983). Some ecological trends in vessel characters. *IAWA Journal*, *4*(2–3), 141–159. https://doi.org/10.1163/22941932-90000407

Ball, M. C. (1996). Comparative ecophysiology of mangrove forest and tropical lowland moist rainforest. In *Tropical forest plant ecophysiology* (pp. 461–496). Springer US. https://doi.org/10.1007/978-1-4613-1163-8_16

Bartoń, K. (2023). Package "MuMIn": Multi-model inference, version 1.47.5.

Beeckman, H. (2016). Wood anatomy and trait-based ecology. *IAWA Journal*, *37*(2), 127–151. https://doi.org/10.1163/22941932-20160127

Bittencourt, P. R., Pereira, L., & Oliveira, R. S. (2016). On xylem hydraulic efficiencies, wood space-use and the safety–efficiency tradeoff. *New Phytologist*, *211*(4), 1152–1155. https://www.jstor.org/stable/newphytologist.211.4.1152

Bittencourt, P. R., Pereira, L., & Oliveira, R. S. (2018). Pneumatic method to measure plant xylem embolism. *Bio-Protocol*, *8*(20), e3059. https://doi.org/10.21769/bioprotoc.3059

Bittencourt, P. R. D. L., Bartholomew, D. C., Banin, L. F., Bin Suis, M. A. F., Nilus, R., Burslem, D. F., & Rowland, L. (2022). Divergence of hydraulic traits among tropical forest trees across topographic and vertical environment gradients in Borneo. *New Phytologist*, *235*(6), 2183–2198. https://doi.org/10.1111/nph.18280

Blackman, C. J., & Brodribb, T. J. (2011). Two measures of leaf capacitance: Insights into the water transport pathway and hydraulic conductance in leaves. *Functional Plant Biology*, *38*(2), 118–126. https://doi.org/10.1071/fp10183

Blomberg, S. P., Garland, T., Jr., & Ives, A. R. (2003). Testing for phylogenetic signal in comparative data: Behavioral traits are more labile. *Evolution*, *57*(4), 717–745. https://doi.org/10.1111/j.0014-3820.2003.tb00285.x

Bremner, J. M., & Breitenbeck, G. (1983). A simple method for determination of ammonium in semimicro-Kjeldahl analysis of soils and plant materials using a block digester. *Communications in Soil Science and Plant Analysis*, *14*(10), 905–913. https://doi.org/10.1080/00103628309367418

Bricheno, L. M., Wolf, J., & Sun, Y. (2021). Saline intrusion in the Ganges-Brahmaputra-Meghna mega delta. *Estuarine, Coastal and Shelf Science*, *252*, 107246. https://doi.org/10.1016/j.ecss.2021.107246

Brodribb, T. J., & Cochard, H. (2009). Hydraulic failure defines the recovery and point of death in water-stressed conifers. *Plant Physiology*, *149*(1), 575–584. https://doi.org/10.1104/pp.108.129783

Brum, M., Pereira, L., Ribeiro, R. V., Jansen, S., Bittencourt, P. R., Oliveira, R. S., & Saleska, S. R. (2023). Reconciling discrepancies in measurements of vulnerability to xylem embolism with the pneumatic method. *New Phytologist*, *237*(2), 374–383. https://doi.org/10.1111/nph.18531

Burnham, K. P., & Anderson, D. R. (2002). *Model selection and multimodel inference: A practical information-theoretic approach*. Springer New York. https://doi.org/10.2307/3802723

Carlquist, S. (2009). Non-random vessel distribution in woods: Patterns, modes, diversity, correlations. *Aliso: A Journal of Systematic and Floristic Botany*, *27*(1), 39–58. https://doi.org/10.5642/aliso.20092701.04

Carlquist, S. (2012). How wood evolves: A new synthesis. *Botany*, *90*(10), 901–940. https://doi.org/10.1139/b2012-048

Carlquist, S. (2016). Wood anatomy of Brassicales: New information, new evolutionary concepts. *The Botanical Review*, *82*, 24–90. https://doi.org/10.1007/s12229-016-9161-2

Carlquist, S. (2018). Living cells in wood 3. Overview; functional anatomy of the parenchyma network. *The Botanical Review*, *84*, 242–294. https://doi.org/10.1007/s12229-018-9198-5

Carlquist, S., & Hoekman, D. A. (1985). Ecological wood anatomy of the woody southern Californian flora. *IAWA Journal*, *6*(4), 319–347. https://doi.org/10.1163/22941932-90000960

Carvalho, E. C., Souza, B. C., Silva, M. S., Menezes, B. S., Martins, F. R., Araújo, F. S., & Soares, A. A. (2023). Xylem anatomical traits determine the variation in wood density and water storage of plants in tropical semiarid climate. *Flora*, *298*, 152185. https://doi.org/10.1016/j.flora.2022.152185

Chave, J., Muller-Landau, H. C., Baker, T. R., Easdale, T. A., Steege, H. T., & Webb, C. O. (2006). Regional and phylogenetic variation of wood density across 2456 neotropical tree species. *Ecological Applications*, *16*(6), 2356–2367. https://doi.org/10.1890/1051-0761(2006)016[2356:rapvow]2.0.co;2

Chen, G., Cai, Q., Ma, S., Feng, Y., Fang, W., Ji, C., Zhu, J., Wang, Z., Wang, S., Tang, Z., & Fang, J. (2023). Climate and forest attributes influence above-ground biomass of deciduous broadleaf forests in China. *Journal of Ecology*, *111*(2), 495–508. https://doi.org/10.1111/1365-2745.14042

Chen, Y., & Ye, Y. (2014). Effects of salinity and nutrient addition on mangrove *Excoecaria agallocha*. *PLoS One*, *9*(4), e93337. https://doi.org/10.1371/journal.pone.0093337

Choat, B., Sack, L., & Holbrook, N. M. (2007). Diversity of hydraulic traits in nine Cordia species growing in tropical forests with contrasting precipitation. *New Phytologist*, *175*(4), 686–698. https://doi.org/10.1111/j.1469-8137.2007.02137.x

Chowdhury, M. Q., De Ridder, M., & Beeckman, H. (2016). Climatic signals in tree rings of Heritiera fomes Buch.-Ham. in the Sundarbans, Bangladesh. *PLoS One*, *11*(2), e0149788. https://doi.org/10.1371/journal.pone.0149788

Chowdhury, M. Q., Kitin, P., De Ridder, M., Delvaux, C., & Beeckman, H. (2016). Cambial dormancy induced growth rings in Heritiera fomes Buch.-Ham.: A proxy for exploring the dynamics of Sundarbans, Bangladesh. *Trees*, *30*, 227–239. https://doi.org/10.1007/s00468-015-1292-2

Chowdhury, M. Q., Sarker, S. K., Gupta, A. D., & Datta, A. (2023). Radial growth in mangrove *Xylocarpus granatum* J. Koenig is driven by salinity in the Sundarbans, Bangladesh. *Dendrochronologia*, *79*, 126082. https://doi.org/10.1016/j.dendro.2023.126082

Chowdhury, M. Q., Sarker, S. K., Hossain, S., Imran, M. I. H., & Datta, A. (2024). Salinity regulates radial growth of *Cynometra ramiflora* L. in the Sundarbans mangrove ecosystem. *Dendrochronologia*, *88*, 126270. https://doi.org/10.1016/j.dendro.2024.126270

Chowdhury, M. Q., Sarker, S. K., Imran, M. I. H., Datta, A., Akther, S. K., Ahmed, Z., & Beeckman, H. (2025). Divergence of vessel diameter explains interspecific variation in hydraulic safety to salinity in the Sundarbans mangrove ecosystem [dataset]. *Dryad Digital Repository*. https://doi.org/10.5061/dryad.18931zd74

Chowdhury, M. Q., Sarker, S. K., Sultana, R., Datta, A., Saimun, M. S. R., & Rashid, A. M. (2023). Synergistic effects of climate and salinity on radial growth of *Excoecaria agallocha* L. in the Sundarbans world heritage mangrove ecosystem. *Estuarine, Coastal and Shelf Science*, *280*, 108181. https://doi.org/10.1016/j.ecss.2022.108181

Chowdhury, M. Q., Schmitz, N., Verheydens, A., Sass-Klaassen, U., Koedam, N., & Beeckman, H. (2008). Nature and periodicity of growth rings in two Bangladeshi mangrove species. *IAWA Journal*, *29*(3), 265–276. https://doi.org/10.1163/22941932-90000185

Cochard, H., Badel, E., Herbette, S., Delzon, S., Choat, B., & Jansen, S. (2013). Methods for measuring plant vulnerability to cavitation: A critical review. *Journal of Experimental Botany*, *64*(15), 4779–4791. https://doi.org/10.1093/jxb/ert193

Cosme, L. H., Schietti, J., Costa, F. R., & Oliveira, R. S. (2017). The importance of hydraulic architecture to the distribution patterns of trees in a central Amazonian forest. *New Phytologist*, *215*(1), 113–125. https://doi.org/10.1111/nph.14508

Dasgupta, S., Sobhan, I., & Wheeler, D. (2017). The impact of climate change and aquatic salinization on mangrove species in the Bangladesh Sundarbans. *Ambio*, *46*, 680–694. https://doi.org/10.1007/s13280-017-0911-0

De Deurwaerder, H., Okello, J. A., Koedam, N., Schmitz, N., & Steppe, K. (2016). How are anatomical and hydraulic features of the mangroves *Avicennia marina* and *Rhizophora mucronata* influenced by siltation? *Trees*, *30*, 35–45. https://doi.org/10.1007/s00468-016-1357-x

Felsenstein, J. (1985). Phylogenies and the comparative method. *The American Naturalist*, *125*(1), 1–15. https://doi.org/10.1086/284325

Friess, D. A., Adame, M. F., Adams, J. B., & Lovelock, C. E. (2022). Mangrove forests under climate change in a 2°C world. *WIREs Climate Change*, *13*(4), e792. https://doi.org/10.1002/wcc.792

Gauthey, A., Peters, J. M., López, R., Carins-Murphy, M. R., Rodriguez-Dominguez, C. M., Tissue, D. T., Medlyn, B. E., Brodribb, T. J., & Choat, B. (2022). Mechanisms of xylem hydraulic recovery after drought in *Eucalyptus saligna*. *Plant, Cell & Environment*, *45*(4), 1216–1228. https://doi.org/10.1111/pce.14265

Gee, G. W., & Bauder, J. W. (1986). Particle-size analysis. In *Methods of soil analysis: Part 1 physical and mineralogical methods* (Vol. *5*, pp. 383–411). American Society of Agronomy/Soil Science Society of America. https://doi.org/10.2136/sssabookser5.1.2ed.c15

Gleason, S. M., Westoby, M., Jansen, S., Choat, B., Hacke, U. G., Pratt, R. B., Bhaskar, R., Brodribb, T. J., Bucci, S. J., Cao, K. F., Cochard, H., Delzon, S., Domec, J. C., Fan, Z. X., Feild, T. S., Jacobsen, A. L., Johnson, D. M., Lens, F., Maherali, H., … Zanne, A. E. (2016). Weak tradeoff between xylem safety and xylem-specific hydraulic efficiency across the world's woody plant species. *New Phytologist*, *209*(1), 123–136. https://doi.org/10.1111/nph.13646

Gopal, B., & Chauhan, M. (2018). The transboundary Sundarbans mangroves (India and Bangladesh). In *The Wetland Book: II: Distribution, description, and conservation* (pp. 1733–1742). Springer Netherlands. https://doi.org/10.1007/978-94-007-4001-3_26

Guyot, G., Scoffoni, C., & Sack, L. (2012). Combined impacts of irradiance and dehydration on leaf hydraulic conductance: Insights into vulnerability and stomatal control. *Plant, Cell & Environment*, *35*(5), 857–871. https://doi.org/10.1111/j.1365-3040.2011.02458.x

Hacke, U. G. (2015). The hydraulic architecture of Populus. In *Functional and ecological xylem anatomy* (pp. 103–131). Springer International Publishing. https://doi.org/10.1007/978-3-319-15783-2_4

Hacke, U. G., Sperry, J. S., Pockman, W. T., Davis, S. D., & McCulloh, K. A. (2001). Trends in wood density and structure are linked to prevention of xylem implosion by negative pressure. *Oecologia*, *126*, 457–461. https://doi.org/10.1007/s004420100628

Hacke, U. G., Sperry, J. S., Wheeler, J. K., & Castro, L. (2006). Scaling of angiosperm xylem structure with safety and efficiency. *Tree Physiology*, *26*(6), 689–701. https://doi.org/10.1093/treephys/26.6.689

Hardie, M., & Doyle, R. (2012). Measuring soil salinity. In *Plant salt tolerance: Methods and protocols* (pp. 415–425). Humana Press. https://doi.org/10.1007/978-1-61779-986-0_28

Harun-or-Rashid, S., Biswas, S. R., Boecker, R., & Kruse, M. (2009). Mangrove community recovery potential after catastrophic disturbances in Bangladesh. *Forest Ecology and Management*, *257*(3), 923–930. https://doi.org/10.1016/j.foreco.2008.10.028

Hietz, P., Rosner, S., Hietz-Seifert, U., & Wright, S. J. (2017). Wood traits related to size and life history of trees in a Panamanian rainforest. *New Phytologist*, *213*(1), 170–180. https://doi.org/10.1111/nph.14123

Hossain, M. (2015). Handbook of selected plant species of the Sundarbans and the embankment ecosystem. In *Sustainable development and biodiversity conservation in coastal protection forests, Bangladesh (SDBC-Sundarbans) project* (p. 116). Deutsche Gesellschaft für Internationale Zusammenarbeit (GIZ) GmbH on behalf of the German Federal Ministry for Economic Cooperation and Development (BMZ).

Iftekhar, M. S., & Saenger, P. (2008). Vegetation dynamics in the Bangladesh Sundarbans mangroves: A review of forest inventories. *Wetlands Ecology and Management*, *16*, 291–312. https://doi.org/10.1007/s11273-007-9063-5

Islam, S. N., & Gnauck, A. (2011). Water salinity investigation in the Sundarbans rivers in Bangladesh. *International Journal of Water*, *6*(1–2), 74–91. https://doi.org/10.1504/ijw.2011.043318

Jacobsen, A. L., & Pratt, R. B. (2023). Vessel diameter polymorphism determines vulnerability-to-embolism curve shape. *IAWA Journal*, *44*(3–4), 320–334. https://doi.org/10.1163/22941932-bja10115

Jacobsen, A. L., Pratt, R. B., Ewers, F. W., & Davis, S. D. (2007). Cavitation resistance among 26 chaparral species of southern California. *Ecological Monographs*, *77*(1), 99–115. https://doi.org/10.1890/05-1879

Jacobsen, A. L., Pratt, R. B., Tobin, M. F., Hacke, U. G., & Ewers, F. W. (2012). A global analysis of xylem vessel length in woody plants. *American Journal of Botany*, *99*(10), 1583–1591. https://doi.org/10.3732/ajb.1200140

Janssen, T. A., Hölttä, T., Fleischer, K., Naudts, K., & Dolman, H. (2020). Wood allocation trade-offs between fiber wall, fiber lumen, and axial parenchyma drive drought resistance in neotropical trees. *Plant, Cell & Environment*, *43*(4), 965–980. https://doi.org/10.1111/pce.13687

Jiang, G. F., Brodribb, T. J., Roddy, A. B., Lei, J. Y., Si, H. T., Pahadi, P., Zhang, Y.-J., & Cao, K. F. (2021). Contrasting water use, stomatal regulation, embolism resistance, and drought responses of two co-occurring mangroves. *Water*, *13*(14), 1945. https://doi.org/10.3390/w13141945

Jiang, G. F., Goodale, U. M., Liu, Y. Y., Hao, G. Y., & Cao, K. F. (2017). Salt management strategy defines the stem and leaf hydraulic characteristics of six mangrove tree species. *Tree Physiology*, *37*(3), 389–401. https://doi.org/10.1093/treephys/tpw131

Jiang, G. F., Li, S. Y., Li, Y. C., & Roddy, A. B. (2022). Coordination of hydraulic thresholds across roots, stems, and leaves of two co-occurring mangrove species. *Plant Physiology*, *189*(4), 2159–2174. https://doi.org/10.1093/plphys/kiac240

Kanan, A. H., Pirotti, F., Masiero, M., & Rahman, M. M. (2023). Mapping inundation from sea level rise and its interaction with land cover in the Sundarbans mangrove forest. *Climatic Change*, *176*(8), 104. https://doi.org/10.1007/s10584-023-03574-5

Kondoh, S., Yahata, H., Nakashizuka, T., & Kondoh, M. (2006). Interspecific variation in vessel size, growth and drought tolerance of broad-leaved trees in semi-arid regions of Kenya. *Tree Physiology*, *26*(7), 899–904. https://doi.org/10.1093/treephys/26.7.899

Krauss, K. W., Lovelock, C. E., McKee, K. L., López-Hoffman, L., Ewe, S. M., & Sousa, W. P. (2008). Environmental drivers in mangrove establishment and early development: A review. *Aquatic Botany*, *89*(2), 105–127. https://doi.org/10.1016/j.aquabot.2007.12.014

Krauss, K. W., & Osland, M. J. (2020). Tropical cyclones and the organization of mangrove forests: A review. *Annals of Botany*, *125*(2), 213–234. https://doi.org/10.1093/aob/mcz161

Lachenbruch, B., & McCulloh, K. A. (2014). Traits, properties, and performance: How woody plants combine hydraulic and mechanical functions in a cell, tissue, or whole plant. *New Phytologist*, *204*(4), 747–764. https://doi.org/10.1111/nph.13035

Laughlin, D. C., Delzon, S., Clearwater, M. J., Bellingham, P. J., McGlone, M. S., & Richardson, S. J. (2020). Climatic limits of temperate rainforest tree species are explained by xylem embolism resistance among angiosperms but not among conifers. *New Phytologist*, *226*(3), 727–740. https://doi.org/10.1111/nph.16448

Lê, S., Josse, J., & Husson, F. (2008). FactoMineR: An R package for multivariate analysis. *Journal of Statistical Software*, *25*, 1–18.

Lens, F., Gleason, S. M., Bortolami, G., Brodersen, C., Delzon, S., & Jansen, S. (2022). Functional xylem characteristics associated with drought-induced embolism in angiosperms. *New Phytologist*, *236*(6), 2019–2036. https://doi.org/10.1111/nph.18447

Lens, F., Gleason, S. M., Bortolami, G., Brodersen, C., Delzon, S., & Jansen, S. (2023). Comparative anatomy vs mechanistic understanding: How to interpret the diameter-vulnerability link. *IAWA Journal*, *44*(3-4), 368–380.

Lens, F., Sperry, J. S., Christman, M. A., Choat, B., Rabaey, D., & Jansen, S. (2011). Testing hypotheses that link wood anatomy to cavitation resistance and hydraulic conductivity in the genus Acer. *New Phytologist*, *190*(3), 709–723. https://doi.org/10.1111/j.1469-8137.2010.03518.x

Li, S., Lu, S., Wang, J., Chen, Z., Zhang, Y., Duan, J., Liu, P., Wang, X., & Guo, J. (2023). Responses of physiological, morphological and anatomical traits to abiotic stress in woody plants. *Forests*, *14*(9), 1784. https://doi.org/10.3390/f14091784

Lintunen, A., Lindfors, L., Nikinmaa, E., & Hölttä, T. (2017). Xylem diameter changes during osmotic stress, desiccation and freezing in *Pinus sylvestris* and *Populus tremula*. *Tree Physiology*, *37*(4), 491–500. https://doi.org/10.1093/treephys/tpw114

Liu, H., Xu, Q., He, P., Santiago, L. S., Yang, K., & Ye, Q. (2015). Strong phylogenetic signals and phylogenetic niche conservatism in ecophysiological traits across divergent lineages of Magnoliaceae. *Scientific Reports*, *5*(1), 12246. https://doi.org/10.1038/srep12246

Liu, H., Ye, Q., Gleason, S. M., He, P., & Yin, D. (2021). Weak tradeoff between xylem hydraulic efficiency and safety: Climatic seasonality

matters. *New Phytologist*, *229*(3), 1440–1452. https://doi.org/10.1111/nph.16940

Lohbeck, K. T., Riebesell, U., Collins, S., & Reusch, T. B. (2013). Functional genetic divergence in high CO_2 adapted *Emiliania huxleyi* populations. *Evolution*, *67*(7), 1892–1900.

López-Portillo, J., Ewers, F. W., & Angeles, G. (2005). Sap salinity effects on xylem conductivity in two mangrove species. *Plant, Cell & Environment*, *28*, 1285–1292.

Lovelock, C. E., Ball, M. C., Feller, I. C., Engelbrecht, B. M., & Ling Ewe, M. (2006). Variation in hydraulic conductivity of mangroves: Influence of species, salinity, and nitrogen and phosphorus availability. *Physiologia Plantarum*, *127*(3), 457–464. https://doi.org/10.1111/j.1399-3054.2006.00723.x

Lovelock, C. E., Feller, I. C., McKee, K. L., Engelbrecht, B. M., & Ball, M. C. (2004). The effect of nutrient enrichment on growth, photosynthesis and hydraulic conductance of dwarf mangroves in Panama. *Functional Ecology*, *18*(1), 25–33. https://doi.org/10.1046/j.0269-8463.2004.00805.x

Madrid, E. N., Armitage, A. R., & López-Portillo, J. (2014). *Avicennia germinans* (black mangrove) vessel architecture is linked to chilling and salinity tolerance in the Gulf of Mexico. *Frontiers in Plant Science*, *5*, 103614. https://doi.org/10.3389/fpls.2014.00503

Markesteijn, L., Poorter, L., Bongers, F., Paz, H., & Sack, L. (2011). Hydraulics and life history of tropical dry forest tree species: Coordination of species' drought and shade tolerance. *New Phytologist*, *191*(2), 480–495. https://doi.org/10.1111/j.1469-8137.2011.03708.x

Mauseth, J. D., & Plemons-Rodriguez, B. J. (1998). Evolution of extreme xeromorphic characters in wood: A study of nine evolutionary lines in Cactaceae. *American Journal of Botany*, *85*(2), 209–218. https://doi.org/10.2307/2446308

McCulloh, K. A., & Sperry, J. S. (2005). Patterns in hydraulic architecture and their implications for transport efficiency. *Tree Physiology*, *25*(3), 257–267. https://doi.org/10.1093/treephys/25.3.257

McCulloh, K. A., Sperry, J. S., & Adler, F. R. (2004). Murray's law and the hydraulic vs mechanical functioning of wood. *Functional Ecology*, *18*, 931–938. https://doi.org/10.1111/j.0269-8463.2004.00913.x

McDowell, N., Pockman, W. T., Allen, C. D., Breshears, D. D., Cobb, N., Kolb, T., Plaut, J., Sperry, J., West, A., Williams, D. G., & Yepez, E. A. (2008). Mechanisms of plant survival and mortality during drought: Why do some plants survive while others succumb to drought? *New Phytologist*, *178*(4), 719–739. https://doi.org/10.1111/j.1469-8137.2008.02436.x

Meinzer, F. C., McCulloh, K. A., Lachenbruch, B., Woodruff, D. R., & Johnson, D. M. (2010). The blind men and the elephant: The impact of context and scale in evaluating conflicts between plant hydraulic safety and efficiency. *Oecologia*, *164*, 287–296. https://doi.org/10.1007/s00442-010-1734-x

Mitra, A., & Zaman, S. (2016). Producers of the marine and estuarine ecosystems. In *Basics of Marine and Estuarine Ecology* (pp. 137–192). Springer. https://doi.org/10.1007/978-81-322-2707-6_5

Mrad, A., Johnson, D. M., Love, D. M., & Domec, J. C. (2021). The roles of conduit redundancy and connectivity in xylem hydraulic functions. *New Phytologist*, *231*(3), 996–1007. https://doi.org/10.1111/nph.17429

Nguyen, H. T., Meir, P., Sack, L., Evans, J. R., Oliveira, R. S., & Ball, M. C. (2017). Leaf water storage increases with salinity and aridity in the mangrove *Avicennia marina*: Integration of leaf structure, osmotic adjustment and access to multiple water sources. *Plant, Cell & Environment*, *40*, 1576–1591. https://doi.org/10.1111/pce.12962

Okello, J. A., Schmitz, N., Beeckman, H., Dahdouh-Guebas, F., Kairo, J. G., Koedam, N., & Robert, E. M. (2017). Hydraulic conductivity and xylem structure of partially buried mangrove tree species. *Plant and Soil*, *417*, 141–154. https://doi.org/10.1007/s11104-017-3247-4

Oliveira, R. S., Costa, F. R., van Baalen, E., de Jonge, A., Bittencourt, P. R., Almanza, Y., Barros, F. V., Cordoba, E. C., Fagundes, M. V., Garcia, S., Guimaraes, Z. T. M., Hertel, M., Schietti, J., Rodrigues-Souza, J., & Poorter, L. (2019). Embolism resistance drives the distribution of Amazonian rainforest tree species along hydro-topographic gradients. *New Phytologist*, *221*(3), 1457–1465. https://doi.org/10.1111/nph.15463

Oliveira, R. S., Eller, C. B., Barros, F. D. V., Hirota, M., Brum, M., & Bittencourt, P. (2021). Linking plant hydraulics and the fast–slow continuum to understand resilience to drought in tropical ecosystems. *New Phytologist*, *230*(3), 904–923. https://doi.org/10.1111/nph.17266

Olson, M. E., Anfodillo, T., Rosell, J. A., Petit, G., Crivellaro, A., Isnard, S., León-Gómez, C., Alvarado-Cárdenas, L. O., & Castorena, M. (2014). Universal hydraulics of the flowering plants: Vessel diameter scales with stem length across angiosperm lineages, habits and climates. *Ecology Letters*, *17*(8), 988–997. https://doi.org/10.1111/ele.12302

Onoda, Y., Richards, A. E., & Westoby, M. (2010). The relationship between stem biomechanics and wood density is modified by rainfall in 32 Australian woody plant species. *New Phytologist*, *185*(2), 493–501. https://doi.org/10.1111/j.1469-8137.2009.03088.x

Parker, G. G., Harmon, M. E., Lefsky, M. A., Chen, J., Pelt, R. V., Weis, S. B., Thomas, S. C., Winner, W. E., Shaw, D. C., & Frankling, J. F. (2004). Three-dimensional structure of an old-growth *Pseudotsuga-Tsuga* canopy and its implications for radiation balance, microclimate, and gas exchange. *Ecosystems*, *7*, 440–453. https://doi.org/10.1007/s10021-004-0136-5

Pittermann, J., Sperry, J. S., Wheeler, J. K., Hacke, U. G., & Sikkema, E. H. (2006). Mechanical reinforcement of tracheids compromises the hydraulic efficiency of conifer xylem. *Plant, Cell & Environment*, *29*(8), 1618–1628. https://doi.org/10.1111/j.1365-3040.2006.01539.x

Plavcová, L., & Hacke, U. G. (2012). Phenotypic and developmental plasticity of xylem in hybrid poplar saplings subjected to experimental drought, nitrogen fertilization, and shading. *Journal of Experimental Botany*, *63*(18), 6481–6491. https://doi.org/10.1093/jxb/ers303

Pockman, W. T., & Sperry, J. S. (2000). Vulnerability to xylem cavitation and the distribution of Sonoran desert vegetation. *American Journal of Botany*, *87*(9), 1287–1299. https://doi.org/10.2307/2656722

Polidoro, B. A., Carpenter, K. E., Collins, L., Duke, N. C., Ellison, A. M., Ellison, J. C., Farnsworth, E. J., Fernando, E. S., Kathiresan, K., Koedam, N. E., Livingstone, S. R., Miyagi, T., Moore, G. E., Ngoc Nam, V., Ong, J. E., Primavera, J. H., Salmo, S. G., Sanciangco, J. C., Sukardjo, S., … Yong, J. W. H. (2010). The loss of species: Mangrove extinction risk and geographic areas of global concern. *PLoS One*, *5*(4), e10095. https://doi.org/10.1371/journal.pone.0010095

Poorter, L., Castilho, C. V., Schietti, J., Oliveira, R. S., & Costa, F. R. (2018). Can traits predict individual growth performance? A test in a hyperdiverse tropical forest. *New Phytologist*, *219*(1), 109–121.

Pratt, R. B., & Jacobsen, A. L. (2017). Conflicting demands on angiosperm xylem: Tradeoffs among storage, transport and biomechanics. *Plant, Cell & Environment*, *40*(6), 897–913. https://doi.org/10.1111/pce.12862

Pratt, R. B., Jacobsen, A. L., Ewers, F. W., & Davis, S. D. (2007). Relationships among xylem transport, biomechanics and storage in stems and roots of nine Rhamnaceae species of the California chaparral. *New Phytologist*, *174*(4), 787–798. https://doi.org/10.1111/j.1469-8137.2007.02061.x

R Core Team. (2023). *R: A language and environment for statistical computing*. R Foundation for Statistical Computing.

Rahman, M. S., Sass-Klaassen, U., Zuidema, P. A., Chowdhury, M. Q., & Beeckman, H. (2020). Salinity drives growth dynamics of the mangrove tree Sonneratia apetala Buch.-Ham. In the Sundarbans, Bangladesh. *Dendrochronologia*, *62*, 125711. https://doi.org/10.1016/j.dendro.2020.125711

Raza, A., Tabassum, J., Fakhar, A. Z., Sharif, R., Chen, H., Zhang, C., Ju, L., Fotopoulos, V., Siddique, K. H. M., Singh, R. K., Zhuang, W., & Varshney, R. K. (2023). Smart reprograming of plants against

salinity stress using modern biotechnological tools. *Critical Reviews in Biotechnology*, *43*(7), 1035–1062. https://doi.org/10.1080/07388551.2022.2093695

Reef, R., Feller, I. C., & Lovelock, C. E. (2010). Nutrition of mangroves. *Tree Physiology*, *30*(9), 1148–1160. https://doi.org/10.1093/treephys/tpq048

Reef, R., & Lovelock, C. E. (2015). Regulation of water balance in mangroves. *Annals of Botany*, *115*(3), 385–395. https://doi.org/10.1093/aob/mcu174

Revell, L. J. (2012). phytools: An R package for phylogenetic comparative biology (and other things). *Methods in Ecology and Evolution*, *2*, 217–223. https://doi.org/10.1111/j.2041-210x.2011.00169.x

Robert, E. M., Koedam, N., Beeckman, H., & Schmitz, N. (2009). A safe hydraulic architecture as wood anatomical explanation for the difference in distribution of the mangroves Avicennia and Rhizophora. *Functional Ecology*, *23*, 649–657. https://doi.org/10.1111/j.1365-2435.2009.01551.x

Rosas, T., Mencuccini, M., Barba, J., Cochard, H., Saura-Mas, S., & Martínez-Vilalta, J. (2019). Adjustments and coordination of hydraulic, leaf and stem traits along a water availability gradient. *New Phytologist*, *223*(2), 632–646. https://doi.org/10.1111/nph.15684

Sarker, S. K., Matthiopoulos, J., Mitchell, S. N., Ahmed, Z. U., Al Mamun, M. B., & Reeve, R. (2019). 1980s–2010s: The world's largest mangrove ecosystem is becoming homogeneous. *Biological Conservation*, *236*, 79–91. https://doi.org/10.1016/j.biocon.2019.05.011

Sarker, S. K., Reeve, R., & Matthiopoulos, J. (2021). Solving the fourth-corner problem: Forecasting ecosystem primary production from spatial multispecies trait-based models. *Ecological Monographs*, *91*(3), e01454. https://doi.org/10.1002/ecm.1454

Sarker, S. K., Reeve, R., Thompson, J., Paul, N. K., & Matthiopoulos, J. (2016). Are we failing to protect threatened mangroves in the Sundarbans world heritage ecosystem? *Scientific Reports*, *6*(1), 21234. https://doi.org/10.1038/srep21234

Savva, Y., Koubaa, A., Tremblay, F., & Bergeron, Y. (2010). Effects of radial growth, tree age, climate, and seed origin on wood density of diverse jack pine populations. *Trees*, *24*, 53–65. https://doi.org/10.1007/s00468-009-0378-0

Schenk, H. J., Espino, S., Goedhart, C. M., Nordenstahl, M., Cabrera, H. I. M., & Jones, C. S. (2008). Hydraulic integration and shrub growth form linked across continental aridity gradients. *Proceedings of the National Academy of Sciences of the United States of America*, *105*(32), 11248–11253. https://doi.org/10.1073/pnas.0804294105

Schindelin, J., Arganda-Carreras, I., Frise, E., Kaynig, V., Longair, M., Pietzsch, T., Preibisch, S., Rueden, C., Saalfeld, S., Schmid, B., Tinevez, J. Y., White, D. J., Hartenstein, V., Eliceiri, K., Tomancak, P., & Cardona, A. (2012). Fiji: An open-source platform for biological-image analysis. *Nature Methods*, *9*(7), 676–682. https://doi.org/10.1038/nmeth.2019

Schmitz, N., Jansen, S., Verheyden, A., Kairo, J. G., Beeckman, H., & Koedam, N. (2007). Comparative anatomy of intervessel pits in two mangrove species growing along a natural salinity gradient in Gazi Bay, Kenya. *Annals of Botany*, *100*(2), 271–281. https://doi.org/10.1093/aob/mcm103

Schmitz, N., Egerton, J. J. G., Lovelock, C. E., & Ball, M. C. (2012a). Light-dependent maintenance of hydraulic function in mangrove branches: Do xylary chloroplasts play a role in embolism repair? *New Phytologist*, *195*(1), 40–46. https://doi.org/10.1111/j.1469-8137.2012.04187.x

Schmitz, N., Koch, G., Beeckman, H., Koedam, N., Robert, E. M. R., & Schmitt, U. (2012b). A structural andcompositional analysis of intervessel pit membranes in the sapwood of somemangrove woods. *IAWA Journal*, *33*(3), 243–256. https://doi.org/10.1163/22941932-90000091

Schmitz, N., Verheyden, A., Beeckman, H., Kairo, J. G., & Koedam, N. (2006). Influence of a salinity gradient on the vessel characters of the mangrove species *Rhizophora mucronata*. *Annals of Botany*, *98*(6), 1321–1330. https://doi.org/10.1093/aob/mcl224

Scholz, A., Rabaey, D., Stein, A., Cochard, H., Smets, E., & Jansen, S. (2013). The evolution and function of vessel and pit characters with respect to cavitation resistance across 10 Prunus species. *Tree Physiology*, *33*(7), 684–694. https://doi.org/10.1093/treephys/tpt050

Siddique, M. R. H., Zuidema, P. A., Sass-Klaassen, U., & Chowdhury, M. Q. (2021). Ring width and vessel features of the mangrove *Excoecaria agallocha* L. depend on salinity in the Sundarbans, Bangladesh. *Dendrochronologia*, *68*, 125857. https://doi.org/10.1016/j.dendro.2021.125857

Sobrado, M. A. (2001). Hydraulic properties of a mangrove *Avicennia germinans* as affected by NaCl. *Biologia Plantarum*, *44*, 435–438. https://doi.org/10.1023/A:1012479718305

Sobrado, M. A. (2006). Differential leaf gas exchange responses to salinity and drought in the mangrove tree *Avicecennia germinans* (Avicenniaceae). *Revista de Biología Tropical*, *54*(2), 371–375. https://doi.org/10.15517/rbt.v54i2.13877

Sobrado, M. A. (2007). Relationship of water transport to anatomical features in the mangrove *Laguncularia racemosa* grown under contrasting salinities. *New Phytologist*, *173*(3), 584–591. https://doi.org/10.1111/j.1469-8137.2006.01927.x

Song, S., Ding, Y., Li, W., Meng, Y., Zhou, J., Gou, R., Zhang, C., Ye, S., Saintilan, N., Krauss, K. W., Crooks, S., Lv, S., & Lin, G. (2023). Mangrove reforestation provides greater blue carbon benefit than afforestation for mitigating global climate change. *Nature Communications*, *14*(1), 756. https://doi.org/10.1038/s41467-023-36477-1

Spalding, M. D., & Leal, M. (2021). *The state of the world's mangroves 2021*. Global Mangrove Alliance.

Sperry, J. S., Meinzer, F. C., & McCulloh, K. A. (2008). Safety and efficiency conflicts in hydraulic architecture: Scaling from tissues to trees. *Plant, Cell & Environment*, *31*(5), 632–645. https://doi.org/10.1111/j.1365-3040.2007.01765.x

Sperry, J. S., Nichols, K. L., Sullivan, J. E., & Eastlack, S. E. (1994). Xylem embolism in ring-porous, diffuse-porous, and coniferous trees of northern Utah and interior Alaska. *Ecology*, *75*(6), 1736–1752. https://doi.org/10.2307/1939633

Sperry, J. S., & Tyree, M. T. (1988). Mechanism of water stress-induced xylem embolism. *Plant Physiology*, *88*(3), 581–587. https://doi.org/10.1104/pp.88.3.581

Suzuki, N., Rivero, R. M., Shulaev, V., Blumwald, E., & Mittler, R. (2014). Abiotic and biotic stress combinations. *New Phytologist*, *203*(1), 32–43. https://doi.org/10.1111/nph.12797

Twilley, R. R., & Rivera-Monroy, V. H. (2005). Developing performance measures of mangrove wetlands using simulation models of hydrology, nutrient biogeochemistry, and community dynamics. *Journal of Coastal Research*, *40*, 79–93. http://www.jstor.org/stable/25736617

Tyree, M. T. (2003). Plant hydraulics: The ascent of water. *Nature*, *423*(6943), 923. https://doi.org/10.1038/423923a

Tyree, M. T., & Sperry, J. S. (1989). Vulnerability of xylem to cavitation and embolism. *Annual Review of Plant Biology*, *40*(1), 19–36. https://doi.org/10.1146/annurev.pp.40.060189.000315

Tyree, M. T., & Zimmermann, M. H. (2002). Hydraulic architecture of whole plants and plant performance. In *Xylem Structure and the Ascent of Sap* (pp. 175–214). Springer Berlin Heidelberg. https://doi.org/10.1007/978-3-662-04931-0_6

Ueda, I., & Wada, T. (1970). Determination of inorganic phosphate by the molybdovanadate method in the presence of ATP and some interfering organic bases. *Analytical Biochemistry*, *37*, 169–174. https://doi.org/10.1016/0003-2697(70)90273-3

Venturas, M. D., Pratt, R. B., Jacobsen, A. L., Castro, V., Fickle, J. C., & Hacke, U. G. (2019). Direct comparison of four methods to construct xylem vulnerability curves: Differences among techniques are

linked to vessel network characteristics. *Plant, Cell & Environment*, *42*(8), 2422–2436. https://doi.org/10.1111/pce.13565

Verheyden, A., Kairo, J. G., Beeckman, H., & Koedam, N. (2004). Growth rings, growth ring formation and age determination in the mangrove *Rhizophora mucronata*. *Annals of Botany*, *94*(1), 59–66. https://doi.org/10.1093/aob/mch115

von Arx, G., Kueffer, C., & Fonti, P. (2013). Quantifying plasticity in vessel grouping–added value from the image analysis tool ROXAS. *IAWA Journal*, *34*(4), 433–445.

Wagner, K. R., Ewers, F. W., & Davis, S. D. (1998). Tradeoffs between hydraulic efficiency and mechanical strength in the stems of four co-occurring species of Chaparral shrubs. *Oecologia*, *117*, 53–62. https://doi.org/10.1007/s004420050631

Ward, R. D., Friess, D. A., Day, R. H., & Mackenzie, R. A. (2016). Impacts of climate change on mangrove ecosystems: A region by region overview. *Ecosystem Health and Sustainability*, *2*(4), e01211. https://doi.org/10.1002/ehs2.1211

Webb, C. O., Ackerly, D. D., McPeek, M. A., & Donoghue, M. J. (2002). Phylogenies and community ecology. *Annual Review of Ecology and Systematics*, *33*(1), 475–505. https://doi.org/10.1146/annurev.ecolsys.33.010802.150448

Wood, S. N. (2017). *Generalized additive models: An introduction with R*. Chapman and Hall/CRC. https://doi.org/10.1201/9781315370279

Wood, S. N., & Augustin, N. H. (2002). GAMs with integrated model selection using penalized regression splines and applications to environmental modelling. *Ecological Modelling*, *157*(2–3), 157–177. https://doi.org/10.1016/s0304-3800(02)00193-x

Yachi, S., & Loreau, M. (2007). Does complementary resource use enhance ecosystem functioning? A model of light competition in plant communities. *Ecology Letters*, *10*(1), 54–62. https://doi.org/10.1111/j.1461-0248.2006.00994.x

Yáñez-Espinosa, L., Terrazas, T., & López-Mata, L. (2001). Effects of flooding on wood and bark anatomy of four species in a mangrove forest community. *Trees*, *15*, 91–97. https://doi.org/10.1007/s004680000081

Zaman, A. M., Molla, M. K., Pervin, I. A., Rahman, S. M., Haider, A. S., Ludwig, F., & Franssen, W. (2017). Impacts on river systems under 2°C warming: Bangladesh case study. *Climate Services*, *7*, 96–114. https://doi.org/10.1016/j.cliser.2016.10.002

Zanne, A. E., Westoby, M., Falster, D. S., Ackerly, D. D., Loarie, S. R., Arnold, S. E., & Coomes, D. A. (2010). Angiosperm wood structure: Global patterns in vessel anatomy and their relation to wood density and potential conductivity. *American Journal of Botany*, *97*(2), 207–215. https://doi.org/10.3732/ajb.0900178

Zanne, A. E., Pearse, W. D., Cornwell, W. K., McGlinn, D. J., Wright, I. J., & Uyeda, J. C. (2018). Functional biogeography of angiosperms: Life at the extremes. *New Phytologist*, *218*, 1697–1709. https://doi.org/10.1111/nph.15114

Zhang, Y., & Chen, H. Y. (2015). Individual size inequality links forest diversity and above-ground biomass. *Journal of Ecology*, *103*(5), 1245–1252. https://doi.org/10.1111/1365-2745.12425

Zimmermann, M. H. (2002). The vessel network in the stem. In *Xylem Structure and the Ascent of Sap* (pp. 21–36). Springer Berlin Heidelberg. https://doi.org/10.1007/978-3-662-22627-8_3

How to cite this article: Chowdhury, M. Q., Sarker, S. K., Imran, M. I. H., Datta, A., Akhter, S. K., Ahmed, Z., & Beeckman, H. (2025). Divergence of vessel diameter explains interspecific variation in hydraulic safety to salinity in the Sundarbans mangrove ecosystem. *Functional Ecology*, *39*, 876–896. https://doi.org/10.1111/1365-2435.14751